Stability analysis of biorthogonal multiwavelets whose duals are not in L_2 and its application to local semiorthogonal lifting

Jan Maes Adhemar Bultheel

Department of Computer Science, Katholieke Universiteit Leuven, Belgium

Abstract

Wavelets have been used in a broad range of applications such as image processing, computer graphics and numerical analysis. The lifting scheme provides an easy way to construct wavelet bases on meshes of arbitrary topological type. In this paper we shall investigate the Riesz stability of compactly supported (multi-) wavelet bases that are constructed with the lifting scheme on regularly refined meshes of arbitrary topological type. More particularly we are interested in the Riesz stability of a standard two-step lifted wavelet transform consisting of one prediction step and one update step. The design of the update step is based on stability considerations and can be described as local semiorthogonalization, which is the approach of Lounsbery *et al.* in their groundbreaking paper [26]. Riesz stability is important for several wavelet based numerical algorithms such as compression or Galerkin discretization of variational elliptic problems. In order to compute the exact range of Sobolev exponents for which the wavelets form a Riesz basis one needs to determine the smoothness of the dual system. It might occur that the duals, that are only defined through a refinement relation, do not exist in L_2. By using Fourier techniques we can estimate the range of Sobolev exponents for which the wavelet basis forms a Riesz basis without explicitly using the dual functions. Several examples in one and two dimensions are presented. These examples show that the lifted wavelets are a Riesz basis for a larger range of Sobolev exponents than the corresponding non-updated hierarchical bases but, in general, they do not form a Riesz basis of L_2.

Keywords: biorthogonal wavelets, subdivision, lifting, Riesz stability
AMS(MOS) Classification: 65T60, 42B35, 41A15, 68U05
Corresponding author: jan.maes@cs.kuleuven.be

1 Introduction

The objective of this paper is to determine the range of Sobolev exponents s for which the wavelets, that are derived from a standard two-step lifted wavelet transform consisting of one prediction step and one update step, form a Riesz basis of the fractional Sobolev space $H^s(\mathbb{R}^d)$ ([1]). The design of the update step takes into account stability considerations, i.e. we use local semiorthogonal lifting which is the approach taken in [25, 26, 34, 40, 41]. The prediction step is based on subdivision rules. The lifting construction can be applied to irregular meshes of arbitrary topological type but in our stability analysis we will only investigate whether the shifts and dilates of wavelets around regular vertices form a Riesz basis. Recall that a system generated by $\boldsymbol{\psi} := (\psi_1, \psi_2, \ldots, \psi_r)^T$ is a Riesz basis of $H^s(\mathbb{R}^d)$ if

$$\sum_{l=1}^{r}\sum_{j=0}^{\infty}\sum_{k\in\mathbb{Z}^d}\left|c_{l,k}^j\right|^2 \sim \left\|\sum_{l=1}^{r}\sum_{j=0}^{\infty}\sum_{k\in\mathbb{Z}^d} c_{l,k}^j\psi_l(\mathbf{M}^j\cdot-k)\right\|_{H^s(\mathbb{R}^d)}^2$$

with $\mathbf{M}$ a dilation matrix that describes the geometric refinement. We always mean by $a\sim b$ that $a\lesssim b$ and $a\gtrsim b$ hold, where $a\lesssim b$ means that a can be bounded by a constant multiple of b uniformly in any parameters on which a, b may depend, and $a\gtrsim b$ means $b\lesssim a$.

In [26] Lounsbery *et al.* presented a new class of wavelets, based on subdivision surfaces, that radically extended the class of representable functions. Their method allows to develop subdivision wavelets on compact surfaces of arbitrary topological type. At the same time the realization that translation and dilation are not strictly necessary for the construction of wavelets was also noted independently by Sweldens [36, 37] and by Carnicer *et al.* [3]. Starting from a polyhedral mesh, subdivision schemes recursively subdivide the individual polygons such that the surface converges to a smooth limit surface. Wavelet transforms can be constructed by combining the subdivision process with a vertex manipulation that introduces geometric detail at every subdivision level. This approach is directly related to the prediction step and the update step of the lifting scheme. In Section 2 we review some concepts related to the subdivision wavelets from [26] in terms of the lifting scheme.

Without an update step wavelet functions from the lifting scheme are simply the scaling functions on the next finer level corresponding to the newly introduced vertices. The update step is used to achieve certain properties that the unlifted wavelet functions do not have. A simple update from [37] is to obtain lifted wavelets with N vanishing moments where N is the number of degrees of freedom in the update step. This update step appears to be unstable, as reported in [34] for the one-dimensional case. Another possibility would be to make the wavelets orthogonal with respect to the scaling functions of the previous coarser subdivision level. This is a provably stable update, but the resulting wavelet functions are not locally supported. Hence the wavelet transform requires quadratic time which makes the wavelet transform useless from a practical point of view. In Section 3 we discuss another update method that is known as local semiorthogonalization. This approach has been investigated previously in several papers [25, 26, 34, 40, 41]. We prove that this update method yields stable one-level wavelet transforms.

Although we prove that the update step yields stable one-level wavelet transforms, we do not know whether the complete wavelet transform over all levels is stable. In particular we would like to know the complete range of Sobolev exponents for which the multilevel system is a Riesz basis. This is mathematically interesting on its own, but it can also be motivated from the research on multilevel finite element preconditioners [9, 18, 24, 29, 43], as the energy norm of an elliptic partial differential equation is typically a Sobolev norm. In order to be able to use Fourier techniques we will only consider the shift-dilation invariant setting of a multilevel system, although realistic applications require other settings. In Section 4 we establish a theoretical basis for investigating whether the shifts and dilates of the lifted subdivision wavelets form a Riesz basis of $H^s(\mathbb{R}^d)$. This involves determining the smoothness of the dual system, which is generated by the solution of the dual refinement relation. It might happen that the dual refinement relation does not yield a solution in L_2, so that smoothness of the dual system is not well defined anymore. Our main result here is Theorem 4.4 which provides a way to determine the range of stability without explicit knowledge of the dual functions.

In Section 5 we apply the theoretical framework of the previous sections to some example subdivision schemes, i.e. we create subdivision wavelets and we investigate their stability. We find that the subdivision wavelets enlarge the range of stability compared to the unlifted wavelets, but in general they do not form a Riesz basis of L_2 (i.e. $s = 0$ is not contained in the range of Sobolev exponents for which we have stability). In Section 5.1 we give a detailed treatment of the polyhedral wavelets that were used in [26] for smooth surface compression and multiresolution editing. We also illustrate the performance of these wavelets as preconditioners for second order elliptic problems. Section 5.2 is devoted to piecewise cubic Hermite wavelets on the real line, and in Section 5.3 we investigate subdivision wavelets that arise from a more complicated subdivision scheme: the tangent scheme [39]. In Section 5.4 we briefly discuss a strategy to construct stable wavelets with the lifting scheme on uniform grids. Using this strategy we find connections with other constructions in the literature.

2 Multiresolution analysis based on subdivision

2.1 Subdivision

Subdivision is a powerful tool for the construction of smooth curves and surfaces. The main idea is to start with an initial control polyhedron M^0 and to iteratively refine this polyhedron by inserting new vertices such that the sequence of refined polyhedra $M^1, M^2, \ldots$ converges to some limit surface M^∞. In each subdivision step, the vertices of M^{j+1} are computed as affine combinations of the vertices of M^j,

$$\mathbf{v}^{j+1} = \mathbf{v}^j \mathbf{P}^j. \tag{2.1}$$

In this equation the $\mathbf{v}^j$ are matrices whose i-th column contains the x, y, and z coordinates of vertex i of M^j, and the linear combinations on each level are described by the subdivision matrix $\mathbf{P}^j$.

An important aspect of subdivision is its relation to multiresolution analysis. Subdivision can be used to define a collection of refinable scaling functions. Note that subdivision surfaces can be parameterized over the domain M^0. The refinement step that carries the mesh M^j into the mesh M^{j+1} consists of two substeps: a splitting step and an averaging step. In the splitting step each face of M^j is split into a number of congruent subfaces by introducing new vertices at several positions in the old face and by connecting these new vertices with the old vertices. This gives an auxiliary mesh $\widehat{M}^{j+1}$. Then the averaging step uses local weighted averaging to compute the vertex position of M^{j+1} from the vertex positions of $\widehat{M}^{j+1}$. Hence (2.1) can be written in the form

$$\mathbf{s}^{j+1} = \mathbf{s}^j \mathbf{P}^j, \tag{2.2}$$

where the $\mathbf{s}^j$ are row vectors that contain coefficients that are associated with the corresponding vertices in $\widehat{M}^j$, see Figure 1. We define the scaling function ϕ_k^j as the limit function if we start the subdivision scheme (2.2) on level j with an impulse δ_k, i.e. the set of coefficients at level j are all zeroes except at the k-th vertex where we have a corresponding coefficient that equals one. Moreover these scaling functions satisfy a refinement equation of the form

$$\Phi^j = \mathbf{P}^j \Phi^{j+1}, \tag{2.3}$$

where Φ^j denotes the column vector of the scaling functions ϕ_k^j on level j.

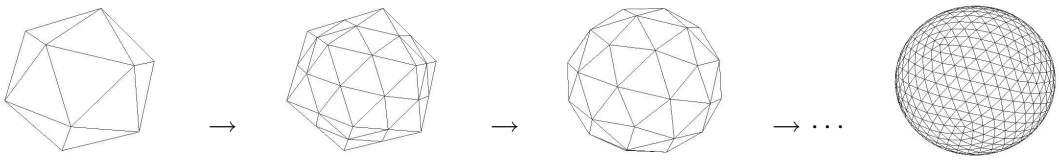

M^0 $\widehat{M}^1$ M^1

Figure 1: The subdivision limiting process.

Given this relation, a strictly increasing sequence of subspaces V^j can be associated with the initial coarse grid M^0:

$$V^j := \operatorname{span}\{\phi_k^j\}$$

and

$$V^0 \subset V^1 \subset V^2 \subset \cdots .$$

This is called a multiresolution analysis.

2.2 Complement space

The space V^{j+1} describes more detail of a surface than the coarser space V^j. The difference can be captured in a complementary space W^j such that

$$V^j \oplus W^j = V^{j+1}.$$

The complement space W^j is not necessarily orthogonal to V^j. We will refer to the basis functions ψ_k^j of W^j as wavelets and we collect them in a column vector Ψ^j. In analogy with (2.3), the relation between Ψ^j and Φ^{j+1} is given by a filter $\mathbf{Q}^j$

$$\Psi^j = \mathbf{Q}^j \Phi^{j+1}.$$

The wavelets are said to have N vanishing moments if W^j is orthogonal to the space of polynomials on M^0 of degree at most $N-1$.

2.3 Filter bank algorithm

Every function in V^{j+1} can be written as a low resolution part in V^j and a detail part in W^j

$$\mathbf{s}^{j+1}\Phi^{j+1} = \mathbf{s}^j \Phi^j + \mathbf{w}^j \Psi^j.$$

This is done with two analysis filters, a low pass filter $\mathbf{A}^j$ and a high pass filter $\mathbf{B}^j$

$$\begin{aligned} \mathbf{s}^j &= \mathbf{s}^{j+1}\mathbf{A}^j \\ \mathbf{w}^j &= \mathbf{s}^{j+1}\mathbf{B}^j. \end{aligned}$$

Since

$$\begin{bmatrix} \Phi^j \\ \Psi^j \end{bmatrix} = \begin{bmatrix} \mathbf{P}^j \\ \mathbf{Q}^j \end{bmatrix} \Phi^{j+1}$$

one can easily see that the analysis filters must be defined by the inverse relation

$$\begin{bmatrix} \mathbf{A}^j & \mathbf{B}^j \end{bmatrix}^{-1} = \begin{bmatrix} \mathbf{P}^j \\ \mathbf{Q}^j \end{bmatrix}$$

and $\mathbf{s}^{j+1}$ can be recovered from $\mathbf{s}^j$ and $\mathbf{w}^j$ using the synthesis filters $\mathbf{P}^j$ and $\mathbf{Q}^j$

$$\mathbf{s}^{j+1} = \mathbf{s}^j \mathbf{P}^j + \mathbf{w}^j \mathbf{Q}^j.$$

The filter operations are represented schematically in Figure 2.

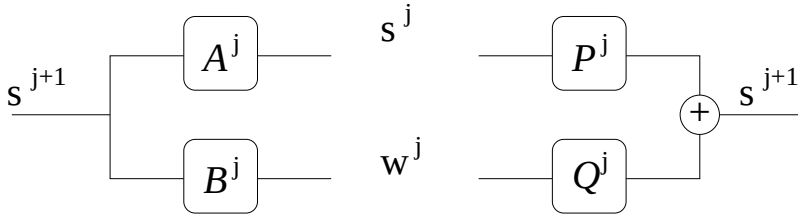

Figure 2: Filter bank algorithm.

2.4 Wavelet functions

The subdivision matrix $\mathbf{P}^j$ can be written in block matrix form as

$$\mathbf{P}^j = \begin{bmatrix} \mathbf{O}^j & \mathbf{N}^j \end{bmatrix}$$

where we distinguish a part $\mathbf{O}^j$ that computes the coefficients that are associated with the old vertices of $\widehat{M}^j$ on the finer domain $\widehat{M}^{j+1}$, and a part $\mathbf{N}^j$ that computes the coefficients that are associated with the newly introduced vertices in $\widehat{M}^{j+1}$. Similarly we split Φ^{j+1} in functions $\mathcal{O}^{j+1}$ associated with the old vertices in $\widehat{M}^{j+1}$ and functions $\mathcal{N}^{j+1}$ associated with the new vertices added when going from $\widehat{M}^j$ to $\widehat{M}^{j+1}$

$$\Phi^{j+1} = \begin{bmatrix} \mathcal{O}^{j+1} \\ \mathcal{N}^{j+1} \end{bmatrix}.$$

The sets Φ^j and $\mathcal{N}^{j+1}$ together span V^{j+1} because the matrix $\mathbf{O}^j$ is invertible. Obviously the functions in $\mathcal{N}^{j+1}$ can be used as wavelet functions

$$\Psi^j = \mathcal{N}^{j+1} \quad \text{and} \quad \mathbf{Q}^j = \begin{bmatrix} \mathbf{0} & \mathbf{I} \end{bmatrix}.$$

Here $\mathbf{0}$ stands for the zero matrix and $\mathbf{I}$ stands for the identity matrix. By choosing the wavelet functions as the scaling functions on the finer level, we also made a choice for the complement space W^j. It can be desirable to have another complement space with certain properties. The wavelet functions can be found by projecting the $\mathcal{N}^{j+1}$ into the desired complement space W^j along V^j

$$\Psi^j = \mathcal{N}^{j+1} - \boldsymbol{\alpha}^j \Phi^j.$$

This projection is not necessarily orthogonal. For each wavelet function there is a corresponding row in $\boldsymbol{\alpha}^j$. The possibly nonzero entries in this row together will be called the stencil for that wavelet function. Remark that if there are no zero entries in $\boldsymbol{\alpha}^j$, the wavelets will have the whole domain M^0 as their support.

2.5 Lifting

The reconstruction or synthesis filter in block matrix form is now

$$\begin{bmatrix} \mathbf{P}^j \\ \mathbf{Q}^j \end{bmatrix} = \begin{bmatrix} \mathbf{O}^j & \mathbf{N}^j \\ -\boldsymbol{\alpha}^j \mathbf{O}^j & \mathbf{I} - \boldsymbol{\alpha}^j \mathbf{N}^j \end{bmatrix}. \tag{2.4}$$

Because $\mathbf{O}^j$ is invertible, the filterbank operation is also easily invertible and we find the analysis filters $\mathbf{A}^j$ and $\mathbf{B}^j$

$$\begin{bmatrix} \mathbf{A}^j & \mathbf{B}^j \end{bmatrix} = \begin{bmatrix} (\mathbf{O}^j)^{-1} - (\mathbf{O}^j)^{-1}\mathbf{N}^j\boldsymbol{\alpha}^j & -(\mathbf{O}^j)^{-1}\mathbf{N}^j \\ \boldsymbol{\alpha}^j & \mathbf{I} \end{bmatrix}. \tag{2.5}$$

These filters can be factored as follows

$$\begin{bmatrix} \mathbf{P}^j \\ \mathbf{Q}^j \end{bmatrix} = \begin{bmatrix} \mathbf{I} & \mathbf{0} \\ -\boldsymbol{\alpha}^j & \mathbf{I} \end{bmatrix} \cdot \begin{bmatrix} \mathbf{I} & \mathbf{N}^j \\ \mathbf{0} & \mathbf{I} \end{bmatrix} \cdot \begin{bmatrix} \mathbf{O}^j & \mathbf{0} \\ \mathbf{0} & \mathbf{I} \end{bmatrix} \tag{2.6}$$

and

$$\begin{bmatrix} \mathbf{A}^j & \mathbf{B}^j \end{bmatrix} = \begin{bmatrix} (\mathbf{O}^j)^{-1} & \mathbf{0} \\ \mathbf{0} & \mathbf{I} \end{bmatrix} \cdot \begin{bmatrix} \mathbf{I} & -\mathbf{N}^j \\ \mathbf{0} & \mathbf{I} \end{bmatrix} \cdot \begin{bmatrix} \mathbf{I} & \mathbf{0} \\ \boldsymbol{\alpha}^j & \mathbf{I} \end{bmatrix}. \tag{2.7}$$

This relates to the concept of lifting [37]. Every factor in the factorization of the filters corresponds to a lifting step. The filter bank factored in lifting steps is shown in Figure 3.

First the coefficients $\mathbf{s}^{j+1}$ are split into two sequences. The first sequence, $\mathbf{s}_o^{j+1}$, contains the coefficients that correspond to vertices in $\widehat{M}^j$, and the second sequence, $\mathbf{s}_n^{j+1}$, contains coefficients that correspond

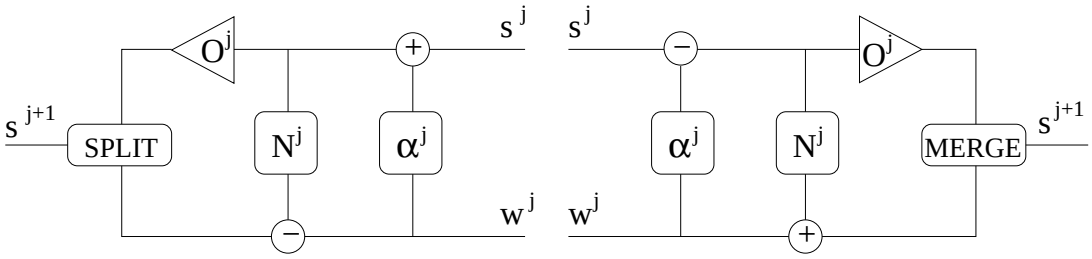

Figure 3: Filter bank factored in lifting steps.

to vertices that are in $\widehat{M}^{j+1}$ but not in $\widehat{M}^{j}$. The subscripts o and n refer to old and new vertices during the subdivision process.

Then we want to treat $\mathbf{s}_o^{j+1}$ as the coefficients of a surface defined on $\widehat{M}^{j}$. Therefore we first need to scale the coefficients of the old vertices with $\mathbf{O}^{j^{-1}}$. After this we can apply the part $\mathbf{N}^j$ of the subdivision algorithm $\mathbf{P}^j$ that leads to the coefficients for the new vertices. The result is used as a prediction for $\mathbf{s}_n^{j+1}$ and substracted from this sequence. This yields the wavelet coefficients $\mathbf{w}^j$ on the lower branch in the picture. We call this step the prediction step. Finally $\mathbf{s}_o^{j+1}$ is updated with a linear combination defined by $\boldsymbol{\alpha}^j$ of wavelet coefficients $\mathbf{w}^j$. This yields the scaling coefficients $\mathbf{s}^j$ on the upper branch in the picture. We call this step the update step.

Reversing the lifting scheme is straightforward: we run through the scheme backwards, replace plus with minus signs, undo scaling operations and merge what had been split. So unlike the classical wavelet transform where $\mathbf{A}^j$, $\mathbf{B}^j$, $\mathbf{P}^j$ and $\mathbf{Q}^j$ are used explicitly, the same filters $\mathbf{O}^j$, $\mathbf{N}^j$ and $\boldsymbol{\alpha}^j$ appear now in the forward and inverse transform.

2.6 Biorthogonal wavelets

The lifting scheme automatically generates a set of biorthogonal scaling functions and wavelets that satisfy a refinement relation of the form

$$\begin{bmatrix} \widetilde{\Phi}^j \\ \widetilde{\Psi}^j \end{bmatrix} = \begin{bmatrix} \left(\mathbf{A}^j\right)^T \\ \left(\mathbf{B}^j\right)^T \end{bmatrix} \widetilde{\Phi}^{j+1}. \tag{2.8}$$

This set of biorthogonal scaling functions and wavelets is only formally biorthogonal. It is not guaranteed that the new dual functions belong to L_2, see [36]. They might only exist in distributional sense in L_2. If the solutions to the refinement equations (2.8) exist in L_2 we have

$$\begin{aligned} \left\langle \widetilde{\phi}_i^j, \phi_{i'}^j \right\rangle_{L_2} &= \delta_{i,i'}, & \left\langle \widetilde{\psi}_k^j, \psi_{k'}^j \right\rangle_{L_2} &= \delta_{k,k'}, \\ \left\langle \widetilde{\phi}_i^j, \psi_k^j \right\rangle_{L_2} &= 0, & \left\langle \widetilde{\psi}_k^j, \phi_i^j \right\rangle_{L_2} &= 0. \end{aligned}$$

3 Design of the update step

Without an update step the multilevel system

$$\boldsymbol{\Psi} := \Phi^0 \cup \bigcup_{j=0}^{\infty} \Psi^j$$

consists of scaling functions on several resolution levels. More particular we have

$$\boldsymbol{\Psi} = \Phi^0 \cup \bigcup_{j=0}^{\infty} \mathcal{N}^j$$

which is just the standard hierarchical basis, see, e.g., [43] for the case where V^j is the space of piecewise linear bivariate polynomials. It is well known that standard hierarchical bases do not form Riesz bases for L_2. For instance they do not have a vanishing moment which is required, [6]. We use the update to achieve properties that the unlifted wavelets do not have.

A common approach is to obtain lifted wavelets with N vanishing moments, where N depends on the size of the update stencil. The lifting coefficients $\boldsymbol{\alpha}^j$ are found as the solution of a $N \times N$ system that arises from the condition that the lifted wavelets are orthogonal to a basis for the space of polynomials on M^0 of degree at most $N-1$. However, the update coefficients in $\boldsymbol{\alpha}^j$ appear to be unbounded, and therefore the wavelet transform is not stable. Simoens [34] gives examples of this phenomenon for the one-dimensional case.

There is another simple update method that is provably stable. One can choose the update operator $\boldsymbol{\alpha}^j$ as the L_2-orthogonal projection from V^{j+1} onto V^j. This yields a multiresolution analysis in which the complement spaces W^j are L_2-orthogonal complements to V^j in V^{j+1}. We will refer to the update as semiorthogonal lifting. Basis functions for these particular complement spaces are sometimes called prewavelets. The resulting multilevel system $\boldsymbol{\Psi}$ is a Riesz basis for L_2 and the wavelets have N vanishing moments provided that V^0 contains the space of polynomials on M^0 of degree at most $N-1$. Unfortunately, in general the matrix $\boldsymbol{\alpha}^j$ is full, so that the lifted wavelets are not locally supported but stretch out over the whole domain M^0. This is a major disadvantage for many applications.

The update matrix $\boldsymbol{\alpha}^j$ for semiorthogonal lifting has an interesting property. Even when $\boldsymbol{\alpha}^j$ is full it has an exponential off-diagonal decay of a rate that is independent of j, see [34] for a proof. Hence the idea of approximating $\boldsymbol{\alpha}^j$ by a truncated matrix [25, 26, 34, 40, 41]. Because of the off-diagonal decay, truncating $\boldsymbol{\alpha}^j$ yields a banded matrix. Local semiorthogonalization exploits this property. One fixes the stencil and the scaling functions that come in the update step in advance and then one orthogonalizes each wavelet function to the subset of V^j that is defined by the stencil. The lifted wavelets will be approximately orthogonal to V^j. A disadvantage of this idea is that we loose all vanishing moments that we had for free in the semiorthogonal case.

Proposition 3.1. *Suppose that the set of scaling functions Φ^j is a Riesz basis of V^j with respect to the L_2-norm, for any $j \geq 0$. Then the set of wavelets Ψ^j, obtained by local semiorthogonal lifting, is a Riesz basis of W^j with respect to the L_2-norm.*

Proof. It is sufficient to show that the one level wavelet transform filters satisfy

$$\left\| \begin{bmatrix} \mathbf{P}^j \\ \mathbf{Q}^j \end{bmatrix} \right\|_2 = \mathcal{O}(1) \quad , \quad \left\| \begin{bmatrix} \mathbf{A}^j & \mathbf{B}^j \end{bmatrix} \right\|_2 = \mathcal{O}(1),$$

uniformly in j. Then, by the Riesz stability of Φ^j, the proposition follows. From (2.6) and (2.7) it is sufficient to prove that $\|\boldsymbol{\alpha}^j\|_2, \|\mathbf{N}^j\|_2, \|\mathbf{O}^j\|_2, \|(\mathbf{O}^j)^{-1}\|_2 = \mathcal{O}(1)$. Because of the Riesz stability of Φ^j one can easily deduce that $\|\mathbf{N}^j\|_2, \|\mathbf{O}^j\|_2, \|(\mathbf{O}^j)^{-1}\|_2 = \mathcal{O}(1)$, using results from [3]. It remains to check whether the update is stable, i.e., $\|\boldsymbol{\alpha}^j\|_2 = \mathcal{O}(1)$. For band matrices with uniformly bounded bandwidth, the 1-norm and the 2-norm are equivalent uniformly in the dimensions of the matrix. Therefore it is sufficient to show that $\|\boldsymbol{\alpha}^j\|_1 \sim \max_{kl} |(\boldsymbol{\alpha}^j)_{kl}|$ is uniformly bounded. Let us focus on the update of a particular wavelet function ψ_k^j where k corresponds to a vertex that is added when going from $\widehat{M}^j$ to $\widehat{M}^{j+1}$. The update involves a set of neighboring scaling functions in V^j. Let us denote these scaling functions by $\{\phi_i^j | i \in I_k\}$, with I_k and index set representing vertices in $\widehat{M}^j$. By construction $\#I_k \lesssim 1$. The update step solves the system

$$\mathbf{G}\boldsymbol{\alpha} = \mathbf{b}, \quad \mathbf{G} := \left(\left\langle \phi_{i_1}^j, \phi_{i_2}^j \right\rangle_{L_2} \right)_{i_1, i_2 \in I_k}, \ \mathbf{b} := \left(\left\langle \phi_i^j, \phi_k^{j+1} \right\rangle_{L_2} \right)_{i \in I_k}. \tag{3.1}$$

Suppose that $\{\vartheta_i^j | i \in I_k\}$ is a dual base for $\{\phi_i^j | i \in I_k\}$, i.e.,

$$\left\langle \vartheta_{i_1}^j, \phi_{i_2}^j \right\rangle_{L_2} = \delta_{i_1, i_2},$$

and suppose that $\vartheta_i^j =: \sum_{n\in I_k} c_{i,n}\phi_n^j$, then $\mathbf{G}^{-1} = (c_{i,n})_{i,n\in I_k}$ and

$$\left\|\vartheta_i^j\right\|_{L_2}^2 = \left\langle \vartheta_i^j, \vartheta_i^j \right\rangle_{L_2} = \left\langle \vartheta_i^j, \sum_{n\in I_k} c_{i,n}\phi_n^j \right\rangle_{L_2} = c_{i,i}.$$

Such a dual basis always exists by the Riesz representation theorem. From the Riesz stability of the scaling functions we get

$$\sum_{n\in I_k} c_{i,n}^2 \lesssim \left\|\vartheta_i^j\right\|_{L_2}^2,$$

thus $\sum_{n\in I_k} c_{i,n}^2 \lesssim c_{i,i}$ and we derive $c_{i,n}^2 \lesssim c_{i,i}$. For $i = n$ this becomes $c_{i,i} \lesssim 1$, hence $|c_{i,n}| \lesssim 1$ and

$$\|\boldsymbol{\alpha}\|_\infty \leq \left\|\mathbf{G}^{-1}\right\|_\infty \|\mathbf{b}\|_\infty \lesssim \|\mathbf{b}\|_\infty \lesssim 1.$$

This proves the proposition. □

Proposition 3.1 does not imply that the multilevel system $\boldsymbol{\Psi}$ is a Riesz basis for L_2. However, the uniform L_2 stability of the wavelets at a fixed resolution level j is a necessary condition to generate a Riesz basis for L_2. Another necessary condition is that the wavelets must have at least one vanishing moment, see for instance [6]. To enforce the vanishing moment one can use a combined approach [25, 26, 34]. One degree of freedom in the update step makes the wavelet orthogonal to polynomials of degree zero. The other degrees of freedom make the wavelet as orthogonal as possible in a least squares sense to its predefined set of scaling functions.

Proposition 3.2. *Suppose that the set of scaling functions Φ^j is a Riesz basis of V^j with respect to the L_2-norm, for any $j \geq 0$. Then the set of wavelets Ψ^j, obtained by local semiorthogonal lifting with an additional linear constraint that forces each wavelet to have a vanishing moment, is a Riesz basis of W^j with respect to the L_2-norm, provided that for any scaling function $\phi_k^{j+1} \in \mathcal{N}^{j+1}$ there exists a scaling function ϕ_m^j in its update stencil such that*

$$\left|\int \phi_k^{j+1} d\omega\right| \lesssim \left|\int \phi_m^j d\omega\right|. \tag{3.2}$$

Proof. The first part of the proof is similar to the proof of Proposition 3.1. It is sufficient to prove that $\max_{kl} |(\boldsymbol{\alpha}^j)_{kl}|$ is uniformly bounded. Instead of (3.1) we now solve the minimization problem

$$\min_{\boldsymbol{\alpha}} \|\mathbf{G}\boldsymbol{\alpha} - \mathbf{b}\|_2 \quad \text{subj. to} \quad \left(\left\langle 1, \phi_i^j \right\rangle_{L_2}\right)_{i\in I_k} \boldsymbol{\alpha} = \left\langle 1, \phi_k^{j+1} \right\rangle_{L_2}, \tag{3.3}$$

with $\mathbf{G}$, $\mathbf{b}$ and I_k as in the proof of Proposition 3.1. We already know that

$$\|\mathbf{G}\|_\infty \lesssim 1, \quad \left\|\mathbf{G}^{-1}\right\|_\infty \lesssim 1, \quad \|\mathbf{b}\|_\infty \lesssim 1. \tag{3.4}$$

Let $\boldsymbol{\varepsilon} := \mathbf{G}\boldsymbol{\alpha} - \mathbf{b}$, then we deduce from (3.4) that

$$\|\boldsymbol{\varepsilon}\|_\infty \lesssim \max\left(\|\boldsymbol{\alpha}\|_\infty, 1\right), \qquad \|\boldsymbol{\alpha}\|_\infty \lesssim \max\left(\|\boldsymbol{\varepsilon}\|_\infty, 1\right). \tag{3.5}$$

Hence if we can find a $\boldsymbol{\alpha}$ such that the vanishing moment condition is satisfied and such that $\|\boldsymbol{\varepsilon}\|_\infty \lesssim 1$, then the minimalization problem (3.3) will always yield a $\|\boldsymbol{\varepsilon}\|_\infty \lesssim 1$, and from (3.5) we get $\|\boldsymbol{\alpha}\|_\infty \lesssim 1$ which proves the proposition. Suppose that we choose $\boldsymbol{\alpha}$ such that all entries $\boldsymbol{\alpha}_i$, $i \in I_k$, are zero, except for one entry $\boldsymbol{\alpha}_m$. From the vanishing moment condition we find

$$\boldsymbol{\alpha}_m = \frac{\left\langle 1, \phi_k^{j+1} \right\rangle_{L_2}}{\left\langle 1, \phi_m^j \right\rangle_{L_2}}.$$

By (3.2), $\|\boldsymbol{\alpha}\|_\infty = |\boldsymbol{\alpha}_m| \lesssim 1$, and (3.5) implies $\|\boldsymbol{\varepsilon}\|_\infty \lesssim 1$. □

Remark 3.3. Condition (3.2) is a weak assumption. Denote by $\{\phi_i^j | i \in I_k\}$ the set of scaling functions in the update stencil of $\phi_k^{j+1} \in \mathcal{N}^{j+1}$ and let $V_k^j = \text{span}\{\phi_i^j | i \in I_k\}$. Denote by $\{\phi_i^{j+1} | i \in J_k\}$ the set of scaling functions at the next finer level whose support is contained in the domain Ω of V_k^j. They span the space V_k^{j+1} and $\phi_k^{j+1} \in V_k^{j+1}$. By the Riesz representation theorem there exist dual Riesz bases $\{\vartheta_i^j | i \in I_k\}$ and $\{\vartheta_i^{j+1} | i \in J_k\}$ such that $V_k^j = \text{span}\{\vartheta_i^j | i \in I_k\}$ and $V_k^{j+1} = \text{span}\{\vartheta_i^{j+1} | i \in J_k\}$. Furthermore the full set of scaling functions in V^j will reproduce polynomials of degree zero, since they are a Riesz basis with respect to the norm in L_2, see, e.g., [33]. Therefore, provided that the space V_k^j is large enough, the orthogonal projection of the constant function onto the space V_k^j will reproduce the constant function exactly in the interior of the domain Ω of V_k^j and will tend to zero near the boundary $\partial\Omega$ of the domain of V_k^j. Similar results hold for V_k^{j+1}. We find that

$$\left\| \sum_{i \in I_k} \left\langle 1, \phi_i^j \right\rangle_{L_2} \vartheta_i^j \right\|_{L_2(\Omega)}^2 \sim \|1\|_{L_2(\Omega)}^2 \sim \left\| \sum_{i \in J_k} \left\langle 1, \phi_i^{j+1} \right\rangle_{L_2} \vartheta_i^{j+1} \right\|_{L_2(\Omega)}^2,$$

and because the dual bases are also Riesz bases,

$$\sum_{i \in I_k} \left\langle 1, \phi_i^j \right\rangle_{L_2}^2 \sim \sum_{i \in J_k} \left\langle 1, \phi_i^{j+1} \right\rangle_{L_2}^2.$$

Since $\#I_k < \#J_k$, this equivalence implies the existence of a scaling function ϕ_m^j in the update stencil of ϕ_k^{j+1} such that (3.2) holds.

4 Stability over all levels

Propositions 3.1 and 3.2 do not imply that the multilevel system $\mathbf{\Psi}$ is a uniformly stable Riesz basis for $L_2(M^0)$. More generally, we are interested in the range of s for which $\mathbf{\Psi}$ forms a Riesz basis for the Sobolev space $H^s(M^0)$. In realistic applications M^0 is a bounded domain of arbitrary topological type such that the nested spaces V^j on M^0 are not shift-dilation invariant. For our stability analysis we will assume a shift-dilation invariant setting for our multilevel system, because this allows us to make use of Fourier techniques. Hence, the main objective of this section is to estimate the range of Sobolev exponents s for which the shifts and dilations of the wavelets, that are derived from the two-step lifted wavelet transform of the previous section around a regular vertex, form a Riesz basis of $H^s(\mathbb{R}^d)$, with d the spatial dimension.

We start with a geometric refinement described by the dilation matrix $\mathbf{M}$ and we suppose that $\mathbf{M}$ is isotropic, i.e. there exists an invertible matrix $\mathbf{\Sigma}$ such that

$$\mathbf{\Sigma M \Sigma}^{-1} = \text{diag}(\sigma_1, \ldots, \sigma_d)$$

with $|\sigma_1| = \cdots = |\sigma_d| = m^{1/d}$, and $m := |\det \mathbf{M}| > 1$. Let $\lambda_k + \mathbf{M}\mathbb{Z}^d$ be the m distinct elements of $\mathbb{Z}^d/(\mathbf{M}\mathbb{Z}^d)$, with $\lambda_0 = 0$. Define the sets

$$\Lambda := \{\lambda_k, k = 0, \ldots, m-1\}, \quad \Lambda' := \Lambda \setminus \{\lambda_0\}.$$

In the most general case we find a multilevel system

$$\mathbf{\Psi} = \{\boldsymbol{\phi}(x - \alpha), m^{j/2} \boldsymbol{\psi}^\lambda(\mathbf{M}^j x - \alpha), \alpha \in \mathbb{Z}^d, j = 0, 1, \ldots, \ \lambda \in \Lambda'\}, \tag{4.1}$$

where

$$\boldsymbol{\phi}(x) := (\phi_1(x), \phi_2(x), \ldots, \phi_r(x))^T, \quad \boldsymbol{\psi}^\lambda(x) := \left(\psi_1^\lambda(x), \psi_2^\lambda(x), \ldots, \psi_r^\lambda(x)\right)^T$$

are $r \times 1$ function vectors on $\mathbb{R}^d$ that satisfy vector refinement equations of the form

$$\boldsymbol{\phi}(x) = \sum_{\alpha \in \mathbb{Z}^d} \mathbf{A}_\alpha \boldsymbol{\phi}(\mathbf{M}x - \alpha), \tag{4.2}$$

$$\boldsymbol{\psi}^\lambda(x) = \sum_{\alpha \in \mathbb{Z}^d} \mathbf{A}_\alpha^\lambda \boldsymbol{\phi}(\mathbf{M}x - \alpha), \tag{4.3}$$

with $\{\mathbf{A}_\alpha\}_\alpha$ and $\{\mathbf{A}_\alpha^\lambda\}_\alpha$ finitely supported sequences of $r \times r$ mask coefficient matrices. By the biorthogonality (2.8) we also have a dual system

$$\widetilde{\boldsymbol{\Psi}} = \{\widetilde{\boldsymbol{\phi}}(x - \alpha), m^{j/2}\widetilde{\boldsymbol{\psi}}^\lambda(\mathbf{M}^j x - \alpha), \alpha \in \mathbb{Z}^d, j = 0, 1, \ldots, \ \lambda \in \Lambda'\}$$

where

$$\widetilde{\boldsymbol{\phi}}(x) = \sum_{\alpha \in \mathbb{Z}^d} \widetilde{\mathbf{A}}_\alpha \widetilde{\boldsymbol{\phi}}(\mathbf{M}x - \alpha), \quad \widetilde{\boldsymbol{\psi}}^\lambda(x) = \sum_{\alpha \in \mathbb{Z}^d} \widetilde{\mathbf{A}}_\alpha^\lambda \widetilde{\boldsymbol{\phi}}(\mathbf{M}x - \alpha). \tag{4.4}$$

It turns out that the range of Sobolev exponents s for which the multilevel system $\boldsymbol{\Psi}$ is a Riesz basis for $H^s(\mathbb{R}^d)$, is determined by the Sobolev regularity of the scaling function vectors $\boldsymbol{\phi}$ and $\widetilde{\boldsymbol{\phi}}$. The Sobolev regularity or smoothness of an arbitrary function f on $\mathbb{R}^d$ is measured by the critical exponent

$$s_f := \sup\left\{s : f \in H^s(\mathbb{R}^d)\right\}$$

and the Sobolev regularity of a function vector is just the infimum of the Sobolev regularities of the functions that it contains. It is known from [7] that if $\boldsymbol{\phi}, \widetilde{\boldsymbol{\phi}} \in L_2(\mathbb{R}^d)$ have compact support, then the multiscale basis $\boldsymbol{\Psi}$ is a Riesz basis for $H^s(\mathbb{R}^d)$ for all s with

$$-s_{\widetilde{\boldsymbol{\phi}}} < s < s_{\boldsymbol{\phi}}$$

and that this interval is sharp. Recently there has been a growing interest in the numerical computation of the smoothness of refinable functions, see, e.g., [4, 19, 32] and references therein. However, a necessary condition in those papers is that the refinable functions exist in L_2. As we have already mentioned in Section 2.6, the duals arising from the lifting scheme do not necessarily satisfy this condition [36]: it is possible that they only exist in distributional sense in L_2. This difficulty was dealt with by Lorentz and Oswald for the single function refinable case (r=1). In their paper [24] they provide sharp stability estimates for systems where the duals do not belong to L_2. We will extend this result to refinable function vectors (i.e for arbitrary $r \geq 1$).

We now introduce a lot of new notation and some theorems to estimate the range of stability for some given multilevel system. Taking the Fourier transform of both sides of (4.2), we obtain

$$\widehat{\boldsymbol{\phi}}(\omega) = P(\mathbf{M}^{-T}\omega)\widehat{\boldsymbol{\phi}}(\mathbf{M}^{-T}\omega), \qquad \omega \in \mathbb{R}^d,$$

and

$$P(\omega) := m^{-1} \sum_{\alpha \in \mathbb{Z}^d} \mathbf{A}_\alpha e^{-i\alpha\cdot\omega}, \qquad \omega \in \mathbb{R}^d,$$

is the symbol associated with (4.2). Here $P(\omega)$ is an $r \times r$ matrix function. Its entries are trigonometric polynomials with real coefficients. It is well-known that if $P(0)$ satisfies Condition E, i.e. 1 is a simple eigenvalue of $P(0)$ and all other eigenvalues of $P(0)$ lie inside the open unit disk, then there exists a unique compactly supported distributional solution vector $\boldsymbol{\phi}(u)$ satisfying (4.2) and $\boldsymbol{\phi}(0) = \mathbf{y}_R$, with $\mathbf{y}_R$ ($\mathbf{y}_L$) the normalized right (left) eigenvector of $P(0)$ associated with eigenvalue 1, see [30]. Without loss of generality we assume that the support of the symbol $P(\omega)$ is in the cube $[-N, N]^d$ for some fixed $N \geq 0$, so $\mathbf{A}_\alpha = \mathbf{0}$ for all $\alpha \notin [-N, N]^d$. Let

$$K := \left(\sum_{j=1}^{\infty} \mathbf{M}^{-j}([-2N, 2N]^d)\right) \cap \mathbb{Z}^d.$$

Define the torus $\mathbb{T} := [0, 2\pi]^d$ and let $C_0(\mathbb{T})^{r\times r}$ denote the space of all $r \times r$ matrix functions with trigonometric polynomial entries. For a given refinement equation with symbol $P(\omega) \in C_0(\mathbb{T})^{r\times r}$ we define the associated transition operator T_P on $C_0(\mathbb{T})^{r\times r}$ by

$$T_P H(\omega) := \sum_{k=0}^{m-1} P(\mathbf{M}^{-T}(\omega + 2\pi\lambda_k))H(\mathbf{M}^{-T}(\omega + 2\pi\lambda_k))P(\mathbf{M}^{-T}(\omega + 2\pi\lambda_k))^*.$$

Define

$$\mathbb{H} := \{H(\omega) \in C_0(\mathbb{T})^{r\times r} : H(\omega) = \sum_{\alpha\in K} \mathbf{H}_\alpha e^{-i\alpha\cdot\omega}\},$$

then $\mathbb{H}$ is invariant under T_P. Furthermore we know from [14, 20] that the eigenfunctions of T_P corresponding to nonzero eigenvalues lie in $\mathbb{H}$. So it is sufficient to consider the restriction of T_P to $\mathbb{H}$ in order to study the eigenvalues and eigenfunctions of T_P. Let us define the refinement operator R_P on $L_2(\mathbb{R}^d)^{r\times 1}$ by

$$R_P F := \sum_{\alpha\in\mathbb{Z}^d} \mathbf{A}_\alpha F(\mathbf{M}\cdot - \alpha),$$

then $\boldsymbol{\phi}$ solves (4.2) if $R_P\boldsymbol{\phi} = \boldsymbol{\phi}$. The cascade algorithm [11] consists in the repeated application of R_P. If for some compactly supported initial $F \in L_2(\mathbb{R}^d)^{r\times 1}$ the cascade algorithm converges in the L_2 norm, then the vector function obtained in the limit is an $L_2(\mathbb{R}^d)^{r\times 1}$-solution of (4.2). The following theorem gives necessary but sufficient conditions to guarantee that (4.2) has a solution in L_2.

Theorem 4.1. *The cascade algorithm associated with the symbol $P(\omega)$ converges in the L_2 norm if and only if $P(\omega)$ satisfies sum rules of order 1, i.e.,*

$$\mathbf{y}_L P(2\pi\mathbf{M}^{-T}\lambda_k) = 0, \quad k = 1, \dots, m-1,$$

and the transition operator T_P satisfies Condition E.

Proofs can be found in [14, 23, 33]. Note that the requirement that $P(\omega)$ satisfies sum rules of order 1 implies that the shifts of the solution $\boldsymbol{\phi}$ of (4.2) reproduce polynomials of degree 0. For the converse to hold true one needs some additional conditions on $\boldsymbol{\phi}$, see [17, Theorem 2.4]. The following theorem is the main result of the paper [19], and it can be used to estimate the smoothness of the solution to (4.2).

Theorem 4.2. *Let $\boldsymbol{\phi} \in L_2(\mathbb{R}^d)^{r\times 1}$ be the normalized solution of (4.2) with symbol $P(\omega)$. Suppose the highest degree of polynomials reproduced by $\boldsymbol{\phi}$ is $k-1$. Let*

$$E_k := \{\eta_l m^{-\mu/d}, \overline{\eta}_l m^{-\mu/d} : |\mu| < k, l = 2, \dots, r\} \cup \{m^{-\mu/d} : |\mu| < 2k\},$$

with $\mu = (\mu_1, \dots, \mu_d) \in \mathbb{N}_0^d$, $m^{-\mu/d} := m^{-\mu_1/d} \cdots m^{-\mu_d/d}$ and $\{\eta_1, \dots, \eta_r\} := \operatorname{spec}(P(0))$, where $\eta_1 = 1$ and $\eta_l \neq 1$ for $l = 2, \dots, r$. Here $\operatorname{spec}(\cdot)$ denotes the spectrum. Define

$$\rho_k := \max\{|\nu| : \nu \in \operatorname{spec}(T_P|_{\mathbb{H}}) \setminus E_k\}.$$

Then

$$s_{\boldsymbol{\phi}} \geq -\frac{d}{2}\log_m \rho_k.$$

If $\boldsymbol{\phi}$ is L_2-stable then we have equality:

$$s_{\boldsymbol{\phi}} = -\frac{d}{2}\log_m \rho_k.$$

One can compute the spectrum of $T_P|_{\mathbb{H}}$ by the formula

$$\operatorname{spec}\left(T_P|_{\mathbb{H}}\right) = \operatorname{spec}\left(b(\mathbf{M}\alpha - \beta)\right)_{\alpha,\beta\in K},$$

where $b(\alpha) := m^{-1}\sum_{\beta\in\mathbb{Z}^d}\overline{\mathbf{A}_\beta}\otimes\mathbf{A}_{\alpha+\beta}$ and $\otimes$ denotes the (right) Kronecker product. The following theorem is due to Dahmen [7].

Theorem 4.3. *Assume that $\boldsymbol{\Psi}$ and $\widetilde{\boldsymbol{\Psi}}$ are dual Riesz bases in $L_2(\mathbb{R}^d)$ with compactly supported basis functions. In particular the symbols $P(\omega)$ and $\widetilde{P}(\omega)$ of the scaling functions $\boldsymbol{\phi}$ resp. $\widetilde{\boldsymbol{\phi}}$ are trigonometric polynomials (i.e. they have finitely supported masks $(\mathbf{A}_\alpha)_\alpha, (\widetilde{\mathbf{A}}_\alpha)_\alpha$). Then the regularity exponents of $\boldsymbol{\phi}$ and $\widetilde{\boldsymbol{\phi}}$ are positive, and*

$$\begin{aligned}\boldsymbol{\Psi} \text{ is a Riesz basis in } H^s(\mathbb{R}^d) &\iff -s_{\widetilde{\boldsymbol{\phi}}} < s < s_{\boldsymbol{\phi}},\\ \widetilde{\boldsymbol{\Psi}} \text{ is a Riesz basis in } H^s(\mathbb{R}^d) &\iff -s_{\boldsymbol{\phi}} < s < s_{\widetilde{\boldsymbol{\phi}}},\end{aligned}$$

where $s_{\boldsymbol{\phi}}$ and $s_{\widetilde{\boldsymbol{\phi}}}$ are the smoothness exponents of $\boldsymbol{\phi}$ resp. $\widetilde{\boldsymbol{\phi}}$.

Theorem 4.3 is not always applicable because it assumes that $\widetilde{\boldsymbol{\phi}} \in L_2(\mathbb{R}^d)^{r\times 1}$, which can be checked by Theorem 4.1. Generally we do not know in advance whether our multilevel system $\boldsymbol{\Psi}$ of the form (4.1) is an L_2 Riesz basis. Therefore, it is possible that the dual system only exists in distributional sense in L_2 which is not sufficient. In that case we cannot use Theorem 4.2 either to compute $s_{\widetilde{\boldsymbol{\phi}}}$. This problem was solved by Lorentz and Oswald in [24] for the case $r = 1$. For the remainder of this section we will treat here the more general case $r \geq 1$ which is a generalization of some of the results in [24]. We prove the following theorem.

Theorem 4.4. *Assume that the scaling function $\boldsymbol{\phi}$ is of compact support, and generates a multiresolution analysis $\boldsymbol{\Psi}$. Assume that the associated dual symbol $\widetilde{P}(\omega)$ is a function vector containing trigonometric polynomials. Furthermore assume that the system $\Phi^0 \cup \Psi^0$ is an L_2-Riesz basis of V^1. If $\widetilde{s} := -\frac{d}{2}\log_m \widetilde{\rho} \leq 0$ satisfies $-\widetilde{s} < s_{\boldsymbol{\phi}}$ with $\widetilde{\rho} := \max\{|\nu| : \nu \in \operatorname{spec}(T_{\widetilde{P}}|_{\mathbb{H}})\}$, then the multilevel system $\boldsymbol{\Psi}$ of the form (4.1) is a Riesz basis in $H^s(\mathbb{R}^d)$ for all s in the interval*

$$-\widetilde{s} < s < s_{\boldsymbol{\phi}}.$$

Furthermore, $\boldsymbol{\Psi}$ is not a Riesz basis in $H^s(\mathbb{R}^d)$ for any $s < -\widetilde{s}$.

First we introduce some notation and we prove some auxiliary lemmas. Suppose that $(\mathbf{c}_\alpha)_\alpha$ is a sequence of $r \times 1$ vectors, then we denote the periodic function vector

$$c(\omega) := \sum_{\alpha\in\mathbb{Z}^d} \mathbf{c}_\alpha e^{-i\alpha\cdot\omega}$$

by the same letter. Likewise we have

$$c^T(\omega) := \sum_{\alpha\in\mathbb{Z}^d} \mathbf{c}_\alpha^T e^{-i\alpha\cdot\omega}.$$

We introduce the matrix function

$$\mathbf{L}(\omega) := \left(P^{\lambda_l}(\omega + 2\pi\mathbf{M}^{-T}\lambda_k)\right)_{k,l\in\Lambda},$$

which is invertible for all $\omega \in \mathbb{T}$ if and only if $\{\boldsymbol{\phi}(x-\alpha), \boldsymbol{\psi}(x-\alpha), \alpha \in \mathbb{Z}^d\}$ is an L_2 Riesz basis in V_1, see [35, Theorem 13]. For our purposes this is satisfied, see Propositions 3.1 and 3.2. From (2.5) and (2.8) we get

$$\mathbf{L}^{-1}(\omega) = \left(\widetilde{P}^{\lambda_k}(\omega + 2\pi\mathbf{M}^{-T}\lambda_l)^*\right)_{k,l\in\Lambda}. \tag{4.5}$$

Lemma 4.5. *Consider the unique decomposition of $v_1 \in V_1$:*

$$v_1 := \sum_{\alpha\in\mathbb{Z}^d} \mathbf{c}_\alpha^T \boldsymbol{\phi}(\mathbf{M}\cdot - \alpha) = v_0 + w_0,$$

with

$$v_0 := \sum_{\beta\in\mathbb{Z}^d} (\mathbf{d}_\beta^{\lambda_0})^T \boldsymbol{\phi}(\cdot - \beta) \in V_0, \qquad w_0 := \sum_{\lambda\in\Lambda'}\sum_{\beta\in\mathbb{Z}^d} (\mathbf{d}_\beta^{\lambda})^T \boldsymbol{\psi}(\cdot - \beta) \in W_0.$$

Then, with

$$\begin{aligned} c(\omega) &:= \sum_{\alpha\in\mathbb{Z}^d} \mathbf{c}_\alpha e^{-i\alpha\cdot\omega}, \\ d^{\lambda_0}(\omega) &:= \sum_{\beta\in\mathbb{Z}^d} \mathbf{d}_\beta^{\lambda_0} e^{-i\beta\cdot\omega}, \end{aligned}$$

we have that

$$d^{\lambda_0}(\mathbf{M}^T\omega) = m^{-1}\sum_{l=0}^{m-1} \widetilde{P}(\omega + 2\pi\mathbf{M}^{-T}\lambda_l)^* c(\omega + 2\pi\mathbf{M}^{-T}\lambda_l). \tag{4.6}$$

Proof. This is a straightforward generalization of Equation (41) in [24]. Some algebra using (4.2) and (4.3) gives

$$v_0 + w_0 = \sum_{\alpha\in\mathbb{Z}^d} \left(\sum_{\lambda\in\Lambda}\sum_{\beta\in\mathbb{Z}^d} (\mathbf{d}_\beta^\lambda)^T \mathbf{A}^\lambda_{\alpha-\mathbf{M}\beta} \right) \boldsymbol{\phi}(\mathbf{M}\cdot - \alpha),$$

with $\mathbf{A}_\alpha^{\lambda_0} := \mathbf{A}_\alpha$. Hence,

$$\mathbf{c}_\alpha^T = \sum_{\lambda\in\Lambda}\sum_{\beta\in\mathbb{Z}^d} (\mathbf{d}_\beta^\lambda)^T \mathbf{A}^\lambda_{\alpha-\mathbf{M}\beta}.$$

Since $\mathbf{M}\beta\cdot\omega = \beta\cdot\mathbf{M}^T\omega$ we infer

$$c^T(\omega) = m\sum_{\lambda\in\Lambda} (d^\lambda)^T(\mathbf{M}^T\omega) P^\lambda(\omega).$$

Substituting the arguments $\omega + 2\pi\mathbf{M}^{-T}\lambda_l$ we get

$$\begin{aligned} \mathbf{C}^T(\omega) &= \left(c^T(\omega + 2\pi\mathbf{M}^{-T}\lambda_l\right)_{l=0}^{m-1} \\ &= m\left(\sum_{k=0}^{m-1} (d^{\lambda_k})^T(\mathbf{M}^T\omega) P^{\lambda_k}(\omega + 2\pi\mathbf{M}^{-T}\lambda_l) \right)_{l=0}^{m-1} \\ &= m\left((d^{\lambda_k})^T(\mathbf{M}^T\omega) \right)_{k=0}^{m-1} \cdot \left(P^{\lambda_k}(\omega + 2\pi\mathbf{M}^{-T}\lambda_l \right)_{k,l=0}^{m-1} \\ &= m\ \mathbf{D}^T(\mathbf{M}^T\omega)\cdot\mathbf{L}^T(\omega), \end{aligned}$$

where $\mathbf{C}^T(\omega)$ and $\mathbf{D}^T(\mathbf{M}^T\omega)$ are $1\times rm$ row vectors. We find that

$$\mathbf{D}(\mathbf{M}^T\omega) = m^{-1}\mathbf{L}^{-1}(\omega)\mathbf{C}(\omega)$$

and (4.6) follows from (4.5). ∎

Let us define the two-level projection $Q_0^1 : V_1 \to V_0$ by

$$Q_0^1 v_1 = v_0, \qquad v_1 \in V_1,$$

where v_1 has a unique decomposition $v_0 + w_0$ with $v_0 \in V_0$ and $w_0 \in W_0$. If the dual system $\widetilde{\mathbf{\Psi}}$ exists in L_2, then this two-level projector can be written as

$$Q_0^1 v_1 = \sum_{\alpha \in \mathbb{Z}^d} \left\langle \widetilde{\boldsymbol{\phi}}(\mathbf{M}^j \cdot - \alpha)^T, v_1 \right\rangle_{L_2} \boldsymbol{\phi}(\mathbf{M}^j \cdot - \alpha).$$

By a dilation argument, we define $Q_j^{j+1} v_{j+1} := Q_0^1(v_{j+1}(\mathbf{M}^{-j}\cdot))(\mathbf{M}^j \cdot)$ for all $v_{j+1} \in V_j$, and $Q_j^{j+k} := Q_j^{j+1} Q_{j+1}^{j+2} \cdots Q_{j+k-1}^{j+k}$. These operators satisfy $Q_j^k Q_{j+1}^k = Q_j^k$ for all $0 \le j < k < \infty$. We also define the following norm on $C_0(\mathbb{T})^{r \times r}$:

$$\left\| T_P^k H \right\|_\infty := \sum_{1 \le i,j \le r} \sup_{\omega \in \mathbb{T}} \left\{ |\mathbf{e}_i^T T_P^k H(\omega) \mathbf{e}_j| \right\},$$

with $\mathbf{e}_i, \mathbf{e}_j$ the i-th resp. j-th column of $\mathbf{I}_r$, and

$$\left\| T_P^k \Big|_{\mathbb{H}} \right\|_\infty := \sup_{H \in \mathbb{H}} \frac{\left\| T_P^k H \right\|_\infty}{\|H\|_\infty}.$$

Lemma 4.6. *For arbitrary $k > 0$ we have the norm equivalence*

$$\left\| Q_j^{j+k} \right\|_{L_2}^2 = \left\| Q_0^k \right\|_{L_2}^2 \sim \left\| T_{\widetilde{P}^*}^k \mathbf{I}_r \right\|_\infty.$$

Proof. First we show that $\left\| Q_0^1 \right\|_{L_2}^2 \sim \left\| T_{\widetilde{P}^*} \mathbf{I}_r \right\|_\infty$. Define v_0, v_1 and w_0 as in Lemma 4.5. Then, by the Riesz basis property of $\{\boldsymbol{\phi}(\mathbf{M}^j \cdot - \alpha), \alpha \in \mathbb{Z}^d\}$ and because $\{e^{i\alpha\cdot\omega}, \alpha \in \mathbb{Z}^d, \omega \in \mathbb{T}\}$ is an orthonormal basis for $L_2(\mathbb{T})$,

$$\left\| Q_0^1 \right\|_{L_2}^2 = \sup_{v_1 \neq 0} \frac{\left\| Q_0^1 v_1 \right\|_{L_2}^2}{\|v_1\|_{L_2}^2} \sim m \sup_{c \neq 0} \frac{\left\| d^{\lambda_0} \right\|_{F(\mathbb{T})}^2}{\|c\|_{F(\mathbb{T})}^2},$$

where

$$\|d\|_{F(\mathbb{T})}^2 := \sum_{1 \le j \le r} \|d_j\|_{L_2(\mathbb{T})}^2$$

is the Frobenius norm of the function vector $d(\omega) = [d_1(\omega) \cdots d_r(\omega)]^T$. Now we use Lemma 4.5 and Hölder's inequality to derive that

$$\begin{aligned}
& m \|d\|_{F(\mathbb{T})}^2 \\
&= m^2 \left\| d(\mathbf{M}^T \cdot) \right\|_{F(\mathbf{M}^{-T}\mathbb{T})}^2 \\
&= \left\| \sum_{k=0}^{m-1} \widetilde{P}(\omega + 2\pi \mathbf{M}^{-T} \lambda_k)^* c(\omega + 2\pi \mathbf{M}^{-T} \lambda_k) \right\|_{F(\mathbf{M}^{-T}\mathbb{T})}^2 \\
&= \sum_{j=1}^r \int_{\mathbf{M}^{-T}\mathbb{T}} \left| \sum_{k=0}^{m-1} \sum_{i=1}^r \widetilde{P}_{ij}(\overline{\omega + 2\pi \mathbf{M}^{-T} \lambda_k}) c_i(\omega + 2\pi \mathbf{M}^{-T} \lambda_k) \right|^2 d\omega \\
&\le \sum_{j=1}^r \int_{\mathbf{M}^{-T}\mathbb{T}} \left(\sum_{k=0}^{m-1} \sum_{i=1}^r \left| \widetilde{P}_{ij}(\overline{\omega + 2\pi \mathbf{M}^{-T} \lambda_k}) \right|^2 \right) \cdot \left(\sum_{k=0}^{m-1} \sum_{i=1}^r \left| c_i(\omega + 2\pi \mathbf{M}^{-T} \lambda_k) \right|^2 \right) d\omega \\
&\le \sum_{j=1}^r \left\| \sum_{k=0}^{m-1} \sum_{i=1}^r \widetilde{P}_{ij}(\overline{\omega + 2\pi \mathbf{M}^{-T} \lambda_k}) \widetilde{P}_{ij}(\omega + 2\pi \mathbf{M}^{-T} \lambda_k) \right\|_{L_\infty(\mathbf{M}^{-T}\mathbb{T})} \\
&\quad \cdot \sum_{i=1}^r \int_{\mathbf{M}^{-T}\mathbb{T}} \left(\sum_{k=0}^{m-1} \left| c_i(\omega + 2\pi \mathbf{M}^{-T} \lambda_k) \right|^2 \right) d\omega
\end{aligned}$$

$$
\begin{aligned}
&= \sum_{j=1}^{r} \left\| \sum_{k=0}^{m-1} \sum_{i=1}^{r} \widetilde{P}_{ji}(\omega + 2\pi \mathbf{M}^{-T}\lambda_k)^* \widetilde{P}_{ij}(\omega + 2\pi \mathbf{M}^{-T}\lambda_k)^{**} \right\|_{L_\infty(\mathbf{M}^{-T}\mathbb{T})} \|c\|^2_{F(\mathbb{T})} \\
&= \sum_{j=1}^{r} \left\| \left[\sum_{k=0}^{m-1} \widetilde{P}(\omega + 2\pi \mathbf{M}^{-T}\lambda_k)^* \widetilde{P}(\omega + 2\pi \mathbf{M}^{-T}\lambda_k)^{**} \right]_{j,j} \right\|_{L_\infty(\mathbf{M}^{-T}\mathbb{T})} \|c\|^2_{F(\mathbb{T})} \\
&\leq \left\| T_{\widetilde{P}^*} \mathbf{I}_r \right\|_\infty \cdot \|c\|^2_{F(\mathbb{T})} .
\end{aligned}
$$

Thus we have $\left\|Q_0^1\right\|_{L_2}^2 \lesssim \left\|T_{\widetilde{P}^*}\mathbf{I}_r\right\|_\infty$. Since Hölder's inequality is a sharp estimate we can find a function vector $c(\omega)$ such that $\left\|Q_0^1\right\|_{L_2}^2 \sim \left\|T_{\widetilde{P}^*}\mathbf{I}_r\right\|_\infty$. To show this equivalence we first prove that, for arbitrary j, there always exists a choice for $c(\omega)$ such that

$$
\int_{\mathbf{M}^{-T}\mathbb{T}} \left| \sum_{k=0}^{m-1} \sum_{i=1}^{r} \widetilde{P}_{ij}(\overline{\omega + 2\pi \mathbf{M}^{-T}\lambda_k}) c_i(\omega + 2\pi \mathbf{M}^{-T}\lambda_k) \right|^2 d\omega = \left\| \left[T_{\widetilde{P}^*}\mathbf{I}_r \right]_{j,j} \right\|_{L_\infty(\mathbb{T})} \|c\|^2_{F(\mathbb{T})} \tag{4.7}
$$

holds. Indeed, choose $c_i(\omega + 2\pi \mathbf{M}^{-T}\lambda_k) = a(\omega)\widetilde{P}_{ij}(\omega + 2\pi \mathbf{M}^{-T}\lambda_k)$ for all $\omega \in \mathbf{M}^{-T}\mathbb{T}$ and $\lambda_k \in \Lambda$, with $a(\omega)$ some measurable function on $\mathbf{M}^{-T}\mathbb{T}$, then

$$
\begin{aligned}
&\int_{\mathbf{M}^{-T}\mathbb{T}} \left| \sum_{k=0}^{m-1} \sum_{i=1}^{r} \widetilde{P}_{ij}(\overline{\omega + 2\pi \mathbf{M}^{-T}\lambda_k}) c_i(\omega + 2\pi \mathbf{M}^{-T}\lambda_k) \right|^2 d\omega \\
&= \int_{\mathbf{M}^{-T}\mathbb{T}} \left(\sum_{k=0}^{m-1} \sum_{i=1}^{r} \left| \widetilde{P}_{ij}(\overline{\omega + 2\pi \mathbf{M}^{-T}\lambda_k}) \right|^2 \right) \cdot \left(\sum_{k=0}^{m-1} \sum_{i=1}^{r} \left| c_i(\omega + 2\pi \mathbf{M}^{-T}\lambda_k) \right|^2 \right) d\omega.
\end{aligned}
$$

Choose $a(\omega)$ as the characteristic function of the set of all $\omega \in \mathbf{M}^{-T}\mathbb{T}$ for which

$$
\sum_{k=0}^{m-1} \sum_{i=1}^{r} \left| \widetilde{P}_{ij}(\overline{\omega + 2\pi \mathbf{M}^{-T}\lambda_k}) \right|^2 \geq (1-\epsilon) \left\| \sum_{k=0}^{m-1} \sum_{i=1}^{r} \left| \widetilde{P}_{ij}(\overline{\omega + 2\pi \mathbf{M}^{-T}\lambda_k}) \right|^2 \right\|_{L_\infty(\mathbf{M}^{-T}\mathbb{T})}
$$

and let $\epsilon \to 0$. Then

$$
\begin{aligned}
&\int_{\mathbf{M}^{-T}\mathbb{T}} \left(\sum_{k=0}^{m-1} \sum_{i=1}^{r} \left| \widetilde{P}_{ij}(\overline{\omega + 2\pi \mathbf{M}^{-T}\lambda_k}) \right|^2 \right) \cdot \left(\sum_{k=0}^{m-1} \sum_{i=1}^{r} \left| c_i(\omega + 2\pi \mathbf{M}^{-T}\lambda_k) \right|^2 \right) d\omega \\
&= \left\| \sum_{k=0}^{m-1} \sum_{i=1}^{r} \left| \widetilde{P}_{ij}(\overline{\omega + 2\pi \mathbf{M}^{-T}\lambda_k}) \right|^2 \right\|_{L_\infty(\mathbf{M}^{-T}\mathbb{T})} \|c\|^2_{F(\mathbb{T})}
\end{aligned}
$$

which implies (4.7). If we treat r as a constant we find that

$$
\left\| T_{\widetilde{P}^*}\mathbf{I}_r \right\|_\infty \cdot \|c\|^2_{F(\mathbb{T})} \sim \max_{1 \leq i,j \leq r} \left\| \left[T_{\widetilde{P}^*}\mathbf{I}_r \right]_{i,j} \right\|_{L_\infty(\mathbb{T})} \|c\|^2_{F(\mathbb{T})} .
$$

By the special symmetric structure of $T_{\widetilde{P}^*}\mathbf{I}_r$ we have that

$$
\max_{1 \leq i,j \leq r} \left\| \left[T_{\widetilde{P}^*}\mathbf{I}_r \right]_{i,j} \right\|_{L_\infty(\mathbb{T})} \|c\|^2_{F(\mathbb{T})} \sim \max_{1 \leq j \leq r} \left\| \left[T_{\widetilde{P}^*}\mathbf{I}_r \right]_{j,j} \right\|_{L_\infty(\mathbb{T})} \|c\|^2_{F(\mathbb{T})} \lesssim m \|d\|^2_{F(\mathbb{T})} ,
$$

and thus $\|Q_0^1\|_{L_2}^2 \sim \|T_{\widetilde{P}^*}\mathbf{I}_r\|_\infty$. By iterating Lemma 4.5 one obtains

$$
\|Q_0^k\|_{L_2}^2 \sim \|T_{\widetilde{P}^*}^k \mathbf{I}_r\|_\infty
$$

in the same way. For the convenience of the reader we present a proof for the case $k = 2$. Let

$$
v_2 := \sum_{\alpha \in \mathbb{Z}^d} (\mathbf{b}_\alpha^{\lambda_0})^T \boldsymbol{\phi}(M^2 \cdot - \alpha) \in V_2, \qquad w_1 := \sum_{\lambda \in \Lambda'} \sum_{\alpha \in \mathbb{Z}^d} (\mathbf{c}_\alpha^{\lambda})^T \boldsymbol{\psi}(M \cdot - \alpha) \in W_1,
$$

so that $v_2 = v_1 + w_1 = v_0 + w_0 + w_1$. From Lemma 4.5 we find

$$\begin{aligned} d^{\lambda_0}(\mathbf{M}^T\omega) &= m^{-1}\sum_{k=0}^{m-1}\widetilde{P}(\omega+2\pi\mathbf{M}^{-T}\lambda_k)^* c^{\lambda_0}(\omega+2\pi\mathbf{M}^{-T}\lambda_k), \\ c^{\lambda_0}(\mathbf{M}^T\omega) &= m^{-1}\sum_{l=0}^{m-1}\widetilde{P}(\omega+2\pi\mathbf{M}^{-T}\lambda_l)^* b^{\lambda_0}(\omega+2\pi\mathbf{M}^{-T}\lambda_l), \end{aligned}$$

and, by substitution,

$$d(\mathbf{M}^{2T}\omega) = m^{-2}\sum_{k,l=0}^{m-1}\widetilde{P}(\mathbf{M}^T\omega+2\pi\mathbf{M}^{-T}\lambda_k)^*\widetilde{P}(\omega_{k,l})^* b^{\lambda_0}(\omega_{k,l})$$

holds, with $\omega_{k,l} := \omega + 2\pi\mathbf{M}^{-T}\lambda_l + 2\pi\mathbf{M}^{-2T}\lambda_k$. For ease of notation we introduce the $r\times r$ matrix

$$S(k,l,\omega) := \widetilde{P}(\omega_{k,l})\widetilde{P}(\mathbf{M}^T\omega+2\pi\mathbf{M}^{-T}\lambda_k),$$

then

$$d(\mathbf{M}^{2T}\omega) = m^{-2}\sum_{k,l=0}^{m-1} S(k,l,\omega)^* b^{\lambda_0}(\omega_{k,l}).$$

Using the same techniques as before we deduce that

$$\begin{aligned} & m^2\|d\|^2_{F(\mathbb{T})} \\ &= m^4\|d(\mathbf{M}^{2T}\cdot)\|^2_{F(\mathbf{M}^{-2T}\mathbb{T})} \\ &= \left\|\sum_{k,l=0}^{m-1} S(k,l,\omega)^* b^{\lambda_0}(\omega_{k,l})\right\|^2_{F(\mathbf{M}^{-2T}\mathbb{T})} \\ &= \sum_{j=1}^{r}\int_{\mathbf{M}^{-2T}\mathbb{T}}\left|\sum_{k,l=0}^{m-1}\sum_{i=1}^{r}\overline{S_{ij}(k,l,\omega)}b_i^{\lambda_0}(\omega_{k,l})\right|^2 d\omega \\ &\le \sum_{j=1}^{r}\int_{\mathbf{M}^{-2T}\mathbb{T}}\left(\sum_{k,l=0}^{m-1}\sum_{i=1}^{r}\left|\overline{S_{ij}(k,l,\omega)}\right|^2\right)\left(\sum_{k,l=0}^{m-1}\sum_{i=1}^{r}\left|b_i^{\lambda_0}(\omega_{k,l})\right|^2\right) d\omega \\ &\le \sum_{j=1}^{r}\left\|\sum_{k,l=0}^{m-1}\sum_{i=1}^{r}\overline{S_{ij}(k,l,\omega)}S_{ij}(k,l,\omega)\right\|_{L_\infty(\mathbf{M}^{-2T}\mathbb{T})}\left\|b^{\lambda_0}\right\|^2_{F(\mathbb{T})} \\ &= \sum_{j=1}^{r}\left\|\sum_{k,l=0}^{m-1}\sum_{i=1}^{r}S_{ji}(k,l,\omega)^*S_{ij}(k,l,\omega)\right\|_{L_\infty(\mathbf{M}^{-2T}\mathbb{T})}\left\|b^{\lambda_0}\right\|^2_{F(\mathbb{T})} \\ &= \sum_{j=1}^{r}\left\|\left[\sum_{k,l=0}^{m-1}S(k,l,\omega)^*S(k,l,\omega)\right]_{j,j}\right\|_{L_\infty(\mathbf{M}^{-2T}\mathbb{T})}\left\|b^{\lambda_0}\right\|^2_{F(\mathbb{T})}. \end{aligned}$$

It is straightforward to check that

$$\begin{aligned} & \sum_{k,l=0}^{m-1} S(k,l,\mathbf{M}^{-2T}\omega)^* S(k,l,\mathbf{M}^{-2T}\omega) \\ &= \sum_{k=0}^{m-1}\widetilde{P}(\mathbf{M}^{-T}(\omega+2\pi\lambda_k))^*\left(T_{\widetilde{P}^*}\mathbf{I}_r\right)\left(\mathbf{M}^{-T}(\omega+2\pi\lambda_k)\right)\widetilde{P}(\mathbf{M}^{-T}(\omega+2\pi\lambda_k))^{**} \end{aligned}$$

$$= \quad T^2_{\widetilde{P}^*}\mathbf{I}_r(\omega).$$

This shows that $\left\|Q_0^2\right\|_{L_2}^2 \lesssim \left\|T^2_{\widetilde{P}^*}\mathbf{I}_r\right\|_\infty$. Similar to the case $k=1$ one can construct a function vector $c(\omega)$ so that the estimates in the derivation above become sharp, hence $\left\|Q_0^2\right\|_{L_2}^2 \sim \left\|T^2_{\widetilde{P}^*}\mathbf{I}_r\right\|_\infty$. This concludes the proof for $k=2$. The lemma follows for general k by iteration. □

Proof of Theorem 4.4. It follows from properties of the spectral radius and Lemma 4.6 that

$$\left\|Q_j^{j+k}v_{j+k}\right\|_{L_2}^2 \lesssim m^{-2\widetilde{s}k/d}\left\|v_{j+k}\right\|_{L_2}^2, \qquad j,k\in\mathbb{N}, \quad v_{j+k}\in V_{j+k}. \tag{4.8}$$

Indeed, we have the equality $\widetilde{\rho} = \lim_{k\to\infty}\left\|(T_{\widetilde{P}}|_{\mathbb{H}})^k\right\|_\infty^{1/k}$. Choose an $\epsilon>0$. The spectral radius of the operator $(\widetilde{\rho}+\epsilon)^{-1}\,T_{\widetilde{P}}|_{\mathbb{H}}$ is strictly smaller than one. Therefore we find that

$$\lim_{k\to\infty}\left\|((\widetilde{\rho}+\epsilon)^{-1}\,T_{\widetilde{P}}|_{\mathbb{H}})^k\right\|_\infty = 0,$$

such that for arbitrary $k>0$ there exists a constant C_ϵ for which

$$\left\|((\widetilde{\rho}+\epsilon)^{-1}\,T_{\widetilde{P}}|_{\mathbb{H}})^k\right\|_\infty < C_\epsilon,$$

or

$$\left\|(T_{\widetilde{P}}|_{\mathbb{H}})^k\right\|_\infty \lesssim (\widetilde{\rho}+\epsilon)^k.$$

Because $\mathbf{I}_r\in\mathbb{H}$ and $\left\|\mathbf{I}_r\right\|_\infty\sim 1$ we find from Lemma 4.6 that

$$\left\|Q_j^{j+k}v_{j+k}\right\|_{L_2}^2 \lesssim (\widetilde{\rho}+\epsilon)^k\left\|v_{j+k}\right\|_{L_2}^2.$$

By definition of $\widetilde{s}$ and by taking a sufficiently small $\epsilon>0$ we find (4.8).

It is well known, see e.g. [29, Lemma 2], that

$$\|f\|_{H^s}^2 \sim \inf_{v_j\in V_j: f=\sum_j v_j}\sum_{j=0}^\infty m^{2js/d}\left\|v_j\right\|_{L_2}^2 \tag{4.9}$$

for all $0<s<s_{\boldsymbol{\phi}}$. Because of the norm equivalence (4.9) it is sufficient to show that

$$\inf_{v_j\in V_j: v_J=\sum_j v_j}\sum_{j=0}^J m^{2js/d}\left\|v_j\right\|_{L_2}^2 \sim \sum_{j=0}^J m^{2js/d}\left\|(Q_j^J - Q_{j-1}^J)v_J\right\|_{L_2}^2$$

for all $-\widetilde{s}<s<s_{\boldsymbol{\phi}}$ which follows from standard techniques as used in [10, 12, 28]. This equivalence implies the H^s Riesz basis property for the finite set

$$\boldsymbol{\Psi}_J := \{\boldsymbol{\phi}(x-\alpha), m^{j(d/2-s)/d}\boldsymbol{\psi}^\lambda(\mathbf{M}^j x-\alpha), \alpha\in\mathbb{Z}^d, j=0,1,\ldots,J,\ \lambda\in\Lambda'\}.$$

Then we let $J\to\infty$ to obtain the H^s Riesz basis property for the (normalized) multilevel system $\boldsymbol{\Psi}$.

Now suppose that $s<-\widetilde{s}$. Let $s'\in(s,-\widetilde{s})$. Similar to the derivation of eq. (4.8) we can now find a sequence $v_J\in V_J$ with $J\to\infty$ such that $\left\|Q_0^J v_J\right\|_{L_2}^2 \gtrsim m^{2s'J/d}\left\|v_J\right\|_{L_2}^2$. Using (4.9) we obtain

$$\|v_J\|_{H^s} \quad\lesssim\quad \inf_{v_j\in V_j: v_J=\sum_j v_j}\sum_{j=0}^J m^{2js/d}\left\|v_j\right\|_{L_2}^2 \lesssim m^{2J(s-s')/d}\left\|Q_0^J v_J\right\|_{L_2}^2$$

$$\lesssim \quad m^{2J(s-s')/d} \left(\left\| Q_0^J v_J \right\|_{L_2}^2 + \sum_{j=1}^{J} m^{2js/d} \left\| (Q_j^J - Q_{j-1}^J) v_J \right\|_{L_2}^2 \right).$$

The factor $m^{2J(s-s')/d}$ goes exponentially fast to zero as $J \to \infty$. Therefore the equivalence

$$\|v_J\|_{H^s} \sim \sum_{j=0}^{J} m^{2js/d} \left\| (Q_j^J - Q_{j-1}^J) v_J \right\|_{L_2}^2$$

does not hold. This establishes Theorem 4.4.

□

Remark 4.7. Q. Jiang and P. Oswald have written MATLAB routines for numerically estimating smoothness exponents, see their papers [21] and [22].

5 Numerical examples

In this section we apply the theoretical framework of the previous sections to some example subdivision schemes. We create subdivision wavelets with the lifting scheme and we investigate their stability. The update method that we use is local semiorthogonalization with or without an additional constraint that enforces a vanishing moment. In most constructions the wavelets are not a Riesz basis of L_2, but they do extend the range of stability when we compare them to the non-updated wavelet system.

5.1 Wavelets from polyhedral subdivision

Polyhedral subdivision converges to the original polyhedron that covers M^0. It does not provide any more than a C^0 continuous surface. Any triangle in the mesh is split into four subtriangles using the midpoints of the edges of the original triangle, see Figure 4.

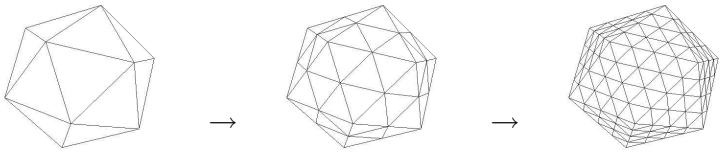

Figure 4: Polyhedral subdivision of an icosahedron.

For each vertex k in the mesh $\widehat{M}^j$ we have a piecewise linear scaling function ϕ_k^j on $\widehat{M}^j$ that takes the value one at vertex k and that is zero at all other vertices, i.e. we simply have the hat functions over $\widehat{M}^j$. Around regular vertices the scaling functions satisfy a refinement equation of the form

$$\boldsymbol{\phi}(x) = \boldsymbol{\phi}(\mathbf{M}x) + \frac{1}{2} \sum_{k \in K_1} \boldsymbol{\phi}(\mathbf{M}x - k),$$

with

$$K_1 := \{(0,1), (1,0), (-1,0), (0,-1), (1,-1), (-1,1)\}$$

and $\mathbf{M} := 2\mathbf{I}_2$. It is well-known that $s_{\boldsymbol{\phi}} = \frac{3}{2}$, but this can also be computed from Theorem 4.2.

If we do not perform an update we simply have the hierarchical basis from [43] which is a Riesz basis for $H^s(\mathbb{R}^2)$ for all $s \in (1, \frac{3}{2})$. To enlarge the range of Sobolev exponents s we update a wavelet at a

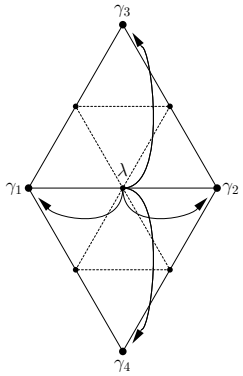

Figure 5: The update stencil for the polyhedral wavelet.

new vertex λ in $\widehat{M}^{j+1}$ by the four old vertices $\gamma_1, \ldots, \gamma_4$ in $\widehat{M}^j$ as in Figure 5. Local semiorthogonal lifting yields

$$\psi_\lambda^j = \phi_\lambda^{j+1} - \frac{11}{60}\left(\phi_{\gamma_1}^j + \phi_{\gamma_2}^j\right) + \frac{1}{60}\left(\phi_{\gamma_3}^j + \phi_{\gamma_4}^j\right)$$

around regular vertices. The dual system satisfies a refinement relation of the form

$$\widetilde{\boldsymbol{\phi}}(x) = \frac{9}{5}\widetilde{\boldsymbol{\phi}}(\mathbf{M}x) + \frac{11}{15}\sum_{k\in K_1}\widetilde{\boldsymbol{\phi}}(\mathbf{M}x-k) - \frac{3}{10}\sum_{k\in K_2}\widetilde{\boldsymbol{\phi}}(\mathbf{M}x-k) - \frac{1}{15}\sum_{k\in K_3}\widetilde{\boldsymbol{\phi}}(\mathbf{M}x-k)$$

with

$$\begin{aligned} K_2 &:= \{(0,2),(2,0),(-2,0),(0,-2),(2,-2),(-2,2)\},\\ K_3 &:= \{(1,1),(-1,-1),(-1,2),(-2,1),(1,-2),(2,-1)\}. \end{aligned}$$

This can be computed from (2.4), (2.5), and (2.8). The dual symbol $\widetilde{P}(\omega)$ satisfies Condition E and we compute in MAPLE that $\widetilde{s} := -\frac{d}{2}\log_m \widetilde{\rho}$ equals $-0.254098...$, with $\widetilde{\rho} := \max\{|\nu| : \nu \in \operatorname{spec}(T_{\widetilde{P}}\big|_{\mathbb{H}})\}$. From Theorem 4.4 we find that the multilevel system $\boldsymbol{\Psi}$ is a Riesz basis for $H^s(\mathbb{R}^2)$ for all $s \in (0.254098..., \frac{3}{2})$. We do not have a Riesz basis for L_2. Figure 6 shows the scaling function and the wavelet function.

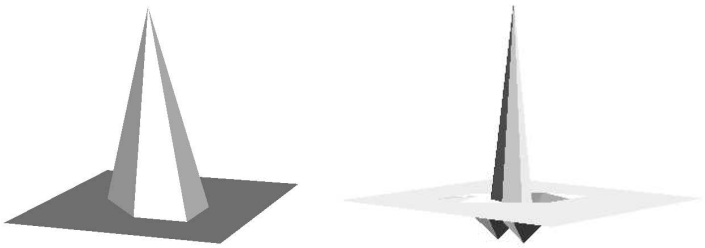

Figure 6: Hat function and corresponding wavelet from local semiorthogonal lifting.

Let us now add a constraint that forces the wavelets to have a vanishing moment. In this case we find that

$$\psi_\lambda^j = \phi_\lambda^{j+1} - \frac{13}{80}\left(\phi_{\gamma_1}^j + \phi_{\gamma_2}^j\right) + \frac{3}{80}\left(\phi_{\gamma_3}^j + \phi_{\gamma_4}^j\right)$$

and

$$\widetilde{\boldsymbol{\phi}}(x) = \frac{41}{20}\widetilde{\boldsymbol{\phi}}(\mathbf{M}x) + \frac{13}{20}\sum_{k\in K_1}\widetilde{\boldsymbol{\phi}}(\mathbf{M}x-k) - \frac{7}{40}\sum_{k\in K_2}\widetilde{\boldsymbol{\phi}}(\mathbf{M}x-k) - \frac{3}{20}\sum_{k\in K_3}\widetilde{\boldsymbol{\phi}}(\mathbf{M}x-k).$$

From Theorem 4.2 we find, using MAPLE, that $s_{\widetilde{\phi}} = 0.328857...$ and the corresponding multilevel system $\mathbf{\Psi}$ is a Riesz basis for $H^s(\mathbb{R}^2)$ for all $s \in (-0.328857..., \frac{3}{2})$, hence we do have a Riesz basis for L_2. Figure 7 shows the wavelet function and the dual scaling function.

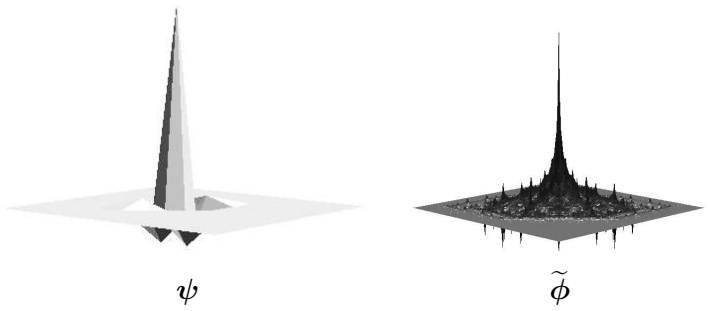

ψ $\qquad$ $\widetilde{\phi}$

Figure 7: Polyhedral wavelet from local semiorthogonal lifting with a linear constraint that enforces a vanishing moment, and the corresponding dual scaling function.

In [40, 41] an approach similar to local semiorthogonal lifting is used to stabilize hierarchical bases. The resulting approximate wavelets are used to precondition linear systems that arise from the Galerkin discretization of second order elliptic partial differential equations. For instance, consider the elliptic problem

$$-\Delta u + qu = f \quad \text{on} \quad \Omega := [0,1]^2, \qquad u|_{\partial\Omega} = 0, \tag{5.1}$$

with $f(x,y) = 2y(1-y) + 2x(1-x) + qx(1-x)y(1-y)$. Then $u(x,y) = x(1-x)y(1-y)$ is the exact solution. The Ritz–Galerkin approximation $u_J \in V^J$ solves

$$a(u_J, v) = \langle f, v \rangle_{L_2}, \quad (v \in V^J),$$

with $a(u,v) := \langle \nabla u, \nabla v \rangle_{L_2} + q \langle u, v \rangle_{L_2}$. Here V^J is the space spanned by the shifts of the standard hat function at resolution level J whose supports are contained in the domain Ω such that the homogeneous boundary conditions are satisfied. Since $a(u,u) \sim \|u\|^2_{H^1(\Omega)}$ for small q, exploiting the polyhedral wavelets leads to uniformly well-conditioned stiffness matrices [9]. If the value of q increases, the zero order term starts to affect stability and we practically have $a(u,u) \sim \|u\|^2_{L_2(\Omega)}$. The polyhedral wavelets should handle this zero order term much better than the standard hierarchical basis, since the wavelets form a Riesz basis of L_2. To solve problem (5.1) we employ a conjugate gradient method and we discretize the problem with the suboptimal hierarchical basis (HB) of Yserentant [43], the polyhedral wavelets with one vanishing moment that we have just derived, and the BPX preconditioner from [2]. Tables 1 and 2 show the results for the cases $q = 1$ resp. $q = 10^8$. For each method we show the number of iterations that are needed to reach the stopping criterion, and the spectral condition number κ of the system matrix for the linear system of equations that is solved. We always take a zero starting vector, and we stop the conjugate gradient iteration if the ℓ_2 norm of the discrete residual is smaller than 10^{-7}.

	BPX		Wavelets		HB	
J	#	κ	#	κ	#	κ
2	13	5.24	16	9.57	16	10.65
3	16	6.99	20	12.66	24	19.64
4	18	8.22	23	14.88	32	32.04
5	20	9.19	25	16.50	39	47.41
6	21	9.97	26	17.74	46	65.74

Table 1: Iteration history for problem (5.1), $q = 1$.

	BPX		Wavelets		HB	
J	#	κ	#	κ	#	κ
2	13	8.25	22	14.62	23	108.24
3	18	12.60	30	19.40	56	607.60
4	21	16.74	34	23.90	120	3.13e+3
5	24	20.76	39	27.74	223	1.53e+4
6	27	24.68	43	31.04	456	7.25e+4

Table 2: Iteration history for problem (5.1), $q = 10^8$.

5.2 Wavelets from Hermite piecewise cubic spline subdivision

Consider the piecewise cubic Hermite splines defined by

$$\phi_1(x) := \begin{cases} (x+1)^2(-2x+1), & x \in [-1,0], \\ (1-x)^2(2x+1), & x \in [0,1] \end{cases}$$
$$\phi_2(x) := \begin{cases} (x+1)^2 x, & x \in [-1,0], \\ (1-x)^2 x, & x \in [0,1] \end{cases},$$

see Figure 8. Integer translates of ϕ_1, ϕ_2 generate the space of C^1 piecewise cubic functions on $\mathbb{R}$

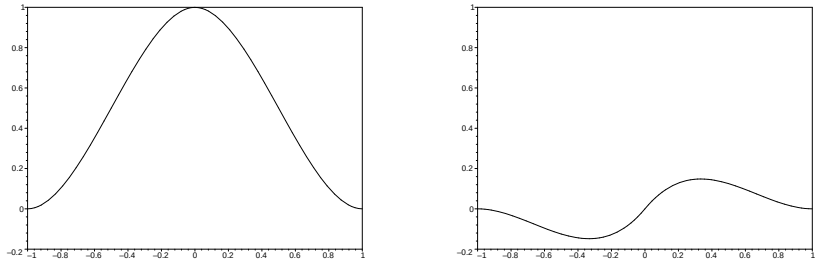

ϕ_1 ϕ_2

Figure 8: Piecewise cubic Hermite splines.

which interpolate function values and first derivatives at the integers. Define the generator $\boldsymbol{\phi}(x) = (\phi_1(x), \phi_2(x))^T$. Then $\boldsymbol{\phi}(x)$ satisfies the refinement equation

$$\boldsymbol{\phi}(x) = \begin{bmatrix} \frac{1}{2} & \frac{3}{4} \\ -\frac{1}{8} & -\frac{1}{8} \end{bmatrix} \boldsymbol{\phi}(2x+1) + \begin{bmatrix} 1 & 0 \\ 0 & \frac{1}{2} \end{bmatrix} \boldsymbol{\phi}(2x) \begin{bmatrix} \frac{1}{2} & -\frac{3}{4} \\ \frac{1}{8} & -\frac{1}{8} \end{bmatrix} \boldsymbol{\phi}(2x-1),$$

and $s_{\boldsymbol{\phi}} = \frac{5}{2}$. The wavelets can be represented by the generator $\boldsymbol{\psi}(x) = (\psi_1(x), \psi_2(x))^T$. We define the update stencil for a new vertex λ in $\widehat{M}^{j+1}$ by the two neighbouring old vertices γ_1 and γ_2 as in Figure 9. Local semiorthogonal lifting gives

$$\boldsymbol{\psi}(x) = \boldsymbol{\phi}(2x-1) - \begin{bmatrix} \frac{491}{2204} & \frac{1989}{1102} \\ \frac{-255}{4484} & \frac{-446}{1121} \end{bmatrix} \boldsymbol{\phi}(x) - \begin{bmatrix} \frac{491}{2204} & \frac{-1989}{1102} \\ \frac{255}{4484} & \frac{-446}{1121} \end{bmatrix} \boldsymbol{\phi}(x-1).$$

Figure 10 depicts the wavelet functions. From (2.4), (2.5), and (2.8) we compute that the dual scaling

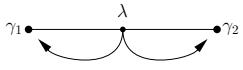

Figure 9: The update stencil for the piecewise cubic Hermite spline wavelet.

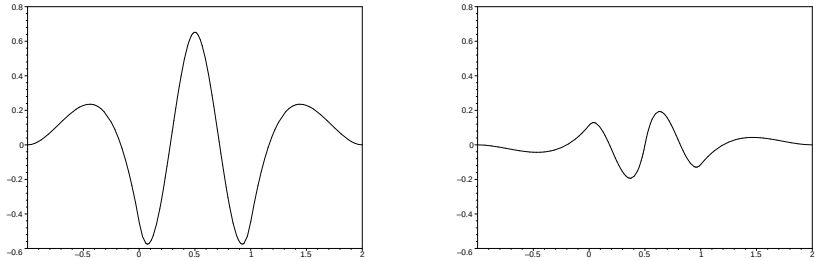

ψ_1 ψ_2

Figure 10: Piecewise cubic Hermite spline wavelets from local semiorthogonal lifting.

functions satisfy a refinement relation of the form

$$\widetilde{\boldsymbol{\phi}}(x) = \begin{bmatrix} \frac{-35753}{260072} & \frac{-10787}{130036} \\ \frac{78549}{65018} & \frac{91483}{130036} \end{bmatrix} \widetilde{\boldsymbol{\phi}}(2x+2) + \begin{bmatrix} \frac{491}{1102} & \frac{255}{2242} \\ \frac{-1989}{551} & \frac{-892}{1121} \end{bmatrix} \widetilde{\boldsymbol{\phi}}(2x+1)$$

$$+ \begin{bmatrix} \frac{9471}{6844} & 0 \\ 0 & \frac{116853}{65018} \end{bmatrix} \widetilde{\boldsymbol{\phi}}(2x) + \begin{bmatrix} \frac{491}{1102} & \frac{-255}{2242} \\ \frac{1989}{551} & \frac{-892}{1121} \end{bmatrix} \widetilde{\boldsymbol{\phi}}(2x-1) + \begin{bmatrix} \frac{-35753}{260072} & \frac{10787}{130036} \\ \frac{-78549}{65018} & \frac{91483}{130036} \end{bmatrix} \widetilde{\boldsymbol{\phi}}(2x-2).$$

The dual symbol $\widetilde{P}(\omega)$ satisfies Condition E and we compute in MAPLE that $\widetilde{s} := -\frac{d}{2}\log_m \widetilde{\rho}$ equals $-0.026490...$, with $\widetilde{\rho} := \max\{|\nu| : \nu \in \operatorname{spec}(T_{\widetilde{P}}\big|_{\mathbb{H}})\}$. From Theorem 4.4 we find that the multilevel system $\boldsymbol{\Psi}$ is a Riesz basis for $H^s(\mathbb{R})$ for all $s \in (0.026490..., \frac{5}{2})$. We do not have a Riesz basis for L_2. If one adds a linear constraint to the update that forces the wavelets to have one vanishing moment one will find that the corresponding dual symbol $\widetilde{P}(\omega)$ does not satisfy Condition E. Hence, the dual functions do not exist in distributional sense in L_2 and Theorem 4.4 is not applicable in this case (one will find that $-\widetilde{s} > s_{\boldsymbol{\phi}}$).

5.3 Wavelets from the tangent scheme

The tangent scheme [38, 39] is a subdivision scheme that yields C^1 continuous surfaces and it is based on uniform Powell–Sabin spline subdivision. For each vertex in $\widehat{M^j}$ we have a control triangle tangent to the subdivision surface instead of a control point. Hence we can associate three scaling functions with each vertex in $\widehat{M^j}$, one for each vertex of the control triangle. The main advantage of this subdivision scheme is that one can choose the values of the tangent vectors in the vertices of the initial polyhedron M^0, see Figure 11. Around regular vertices uniform Powell–Sabin spline subdivision rules [42] are used. Therefore, in the regular regions the three scaling functions that can be associated with a vertex are Powell–Sabin splines [31]. They satisfy a refinement relation of the form (4.2) with $\mathbf{M} := 2\mathbf{I}_2$, and where $\mathbf{A}_{(-1,-1)}$ and $\mathbf{A}_{(0,-1)}$ are given by

$$\frac{1}{4}\begin{bmatrix} 1 & 0 & 2 \\ 0 & 1 & 2 \\ 0 & 0 & 0 \end{bmatrix}, \quad \frac{1}{4}\begin{bmatrix} 1 & 0 & 0 \\ 2 & 0 & 2 \\ 0 & 0 & 1 \end{bmatrix},$$

$\mathbf{A}_{(-1,0)}$, $\mathbf{A}_{(0,0)}$ and $\mathbf{A}_{(1,0)}$ are given by

$$\frac{1}{4}\begin{bmatrix} 0 & 2 & 2 \\ 0 & 1 & 0 \\ 0 & 0 & 1 \end{bmatrix}, \quad \frac{1}{6}\begin{bmatrix} 4 & 1 & 1 \\ 1 & 4 & 1 \\ 1 & 1 & 4 \end{bmatrix}, \quad \frac{1}{4}\begin{bmatrix} 0 & 0 & 0 \\ 2 & 1 & 0 \\ 2 & 0 & 1 \end{bmatrix},$$

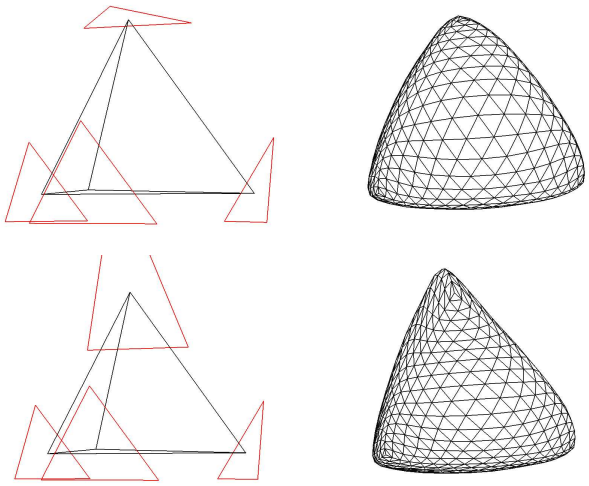

Figure 11: With the tangent scheme the normal on the limit surface in the vertices of the initial polyhedron M^0 can be chosen in advance.

and $\mathbf{A}_{(0,1)}$ and $\mathbf{A}_{(1,1)}$ are given by

$$\frac{1}{4}\begin{bmatrix} 1 & 2 & 0 \\ 0 & 0 & 0 \\ 0 & 2 & 1 \end{bmatrix}, \quad \frac{1}{4}\begin{bmatrix} 1 & 0 & 0 \\ 0 & 1 & 0 \\ 2 & 2 & 0 \end{bmatrix}.$$

One can compute, using MAPLE, that $s_{\boldsymbol{\phi}} = \frac{5}{2}$.

If we do not perform an update we have the hierarchical basis from [27] which is a Riesz basis for $H^s(\mathbb{R}^2)$ for all $s \in (2, \frac{5}{2})$. To enlarge the range of Sobolev exponents s we update the three wavelet functions at a new vertex $\lambda_{12} \in \widehat{M}^{j+1}$ by the six neighbouring coarser scaling functions associated with the vertices γ_1 and γ_2 in $\widehat{M}^j$ as in Figure 12. Local semiorthogonal lifting yields a dual symbol

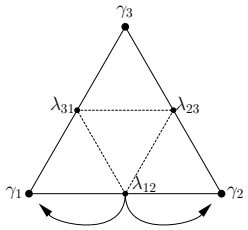

Figure 12: The update stencil for the tangent scheme wavelet.

$\widetilde{P}(\omega)$ that does not satisfy Condition E, hence Theorem 4.4 is not applicable. Local semiorthogonal lifting with a linear constraint that enforces a vanishing moment yields

$$\begin{aligned} \boldsymbol{\psi}^j_{\lambda_{12}} &= \boldsymbol{\phi}^{j+1}_{\lambda_{12}} - \begin{bmatrix} \frac{-10815353}{37042932} & \frac{489004135}{1926232464} & \frac{489004135}{1926232464} \\ \frac{-20302895}{148171728} & \frac{734318841}{4494542416} & \frac{179538083}{3370906812} \\ \frac{-20302895}{148171728} & \frac{179538083}{3370906812} & \frac{734318841}{4494542416} \end{bmatrix} \boldsymbol{\phi}^j_{\gamma_1} \\ &\quad - \begin{bmatrix} \frac{52104049}{481558116} & \frac{-71233997}{1926232464} & \frac{-71233997}{1926232464} \\ \frac{681707773}{1926232464} & \frac{-164964803}{4494542416} & \frac{-247462325}{1685453406} \\ \frac{681707773}{1926232464} & \frac{-247462325}{1685453406} & \frac{-164964803}{4494542416} \end{bmatrix} \boldsymbol{\phi}^j_{\gamma_2} \\ \boldsymbol{\psi}^j_{\lambda_{23}} &= \boldsymbol{\phi}^{j+1}_{\lambda_{23}} - \begin{bmatrix} \frac{734318841}{4494542416} & \frac{-20302895}{148171728} & \frac{179538083}{3370906812} \\ \frac{489004135}{1926232464} & \frac{-10815353}{37042932} & \frac{489004135}{1926232464} \\ \frac{179538083}{3370906812} & \frac{-20302895}{148171728} & \frac{734318841}{4494542416} \end{bmatrix} \boldsymbol{\phi}^j_{\gamma_2} \end{aligned}$$

$$
\begin{aligned}
& - \begin{bmatrix} \frac{-164964803}{4494542416} & \frac{681707773}{1926232464} & \frac{-247462325}{1685453406} \\ \frac{-71233997}{1926232464} & \frac{52104049}{481558116} & \frac{-71233997}{1926232464} \\ \frac{-247462325}{1685453406} & \frac{681707773}{1926232464} & \frac{-164964803}{4494542416} \end{bmatrix} \boldsymbol{\phi}^j_{\gamma_3} \\
\boldsymbol{\psi}^j_{\lambda_{31}} \;=\; & \boldsymbol{\phi}^{j+1}_{\lambda_{31}} - \begin{bmatrix} \frac{734318841}{4494542416} & \frac{179538083}{3370906812} & \frac{-20302895}{148171728} \\ \frac{179538083}{3370906812} & \frac{734318841}{4494542416} & \frac{-20302895}{148171728} \\ \frac{489004135}{1926232464} & \frac{489004135}{1926232464} & \frac{-10815353}{37042932} \end{bmatrix} \boldsymbol{\phi}^j_{\gamma_3} \\
& - \begin{bmatrix} \frac{-164964803}{4494542416} & \frac{-247462325}{1685453406} & \frac{681707773}{1926232464} \\ \frac{-247462325}{1685453406} & \frac{-164964803}{4494542416} & \frac{681707773}{1926232464} \\ \frac{-71233997}{1926232464} & \frac{-71233997}{1926232464} & \frac{52104049}{481558116} \end{bmatrix} \boldsymbol{\phi}^j_{\gamma_1}
\end{aligned}
$$

Figure 13 shows a scaling function and a wavelet function.

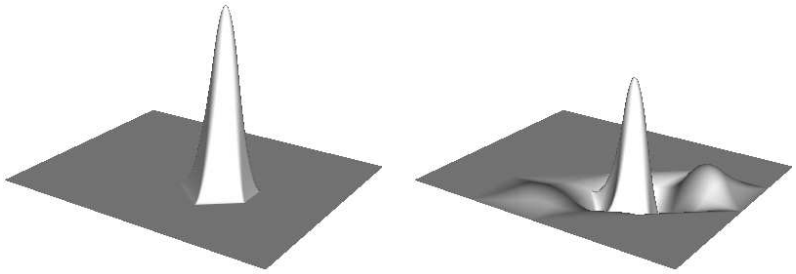

$\phi_1 \in \boldsymbol{\phi}$ $\qquad$ $\psi_1 \in \boldsymbol{\psi}$

Figure 13: Powell–Sabin spline scaling function and corresponding wavelet from local semiorthogonal lifting with a linear constraint that enforces a vanishing moment.

The dual scaling functions satisfy a refinement relation of the form (4.4) where $\widetilde{\mathbf{A}}_{(-2,-2)}$ and $\widetilde{\mathbf{A}}_{(0,-2)}$ are given by

$$
\begin{bmatrix} \frac{-37}{336} & \frac{37}{336} & \frac{-417301265}{642077488} \\ \frac{37}{336} & \frac{-37}{336} & \frac{-417301265}{642077488} \\ 0 & 0 & \frac{20302895}{24695288} \end{bmatrix}, \begin{bmatrix} \frac{1494625759}{13483627248} & \frac{-212816425}{1926232464} & \frac{1488078047}{4494542416} \\ \frac{-366180055}{481558116} & \frac{366180055}{963116232} & \frac{-366180055}{481558116} \\ \frac{1488078047}{4494542416} & \frac{-212816425}{1926232464} & \frac{1494625759}{13483627248} \end{bmatrix},
$$

$\widetilde{\mathbf{A}}_{(-1,-1)}$ and $\widetilde{\mathbf{A}}_{(0,-1)}$ are given by

$$
\begin{bmatrix} \frac{734318841}{1123635604} & \frac{179538083}{842726703} & \frac{489004135}{481558116} \\ \frac{179538083}{842726703} & \frac{734318841}{1123635604} & \frac{489004135}{481558116} \\ \frac{-20302895}{37042932} & \frac{-20302895}{37042932} & \frac{-10815353}{9260733} \end{bmatrix}, \begin{bmatrix} \frac{-164964803}{1123635604} & \frac{-71233997}{481558116} & \frac{-494924650}{842726703} \\ \frac{681707773}{481558116} & \frac{52104049}{120389529} & \frac{681707773}{481558116} \\ \frac{-494924650}{842726703} & \frac{-71233997}{481558116} & \frac{-164964803}{1123635604} \end{bmatrix},
$$

$\widetilde{\mathbf{A}}_{(-2,0)}$, $\widetilde{\mathbf{A}}_{(-1,0)}$, $\widetilde{\mathbf{A}}_{(0,0)}$, $\widetilde{\mathbf{A}}_{(1,0)}$ and $\widetilde{\mathbf{A}}_{(2,0)}$ are given by

$$
\begin{bmatrix} \frac{366180055}{963116232} & \frac{-366180055}{481558116} & \frac{-366180055}{481558116} \\ \frac{-212816425}{1926232464} & \frac{1494625759}{13483627248} & \frac{1488078047}{4494542416} \\ \frac{-212816425}{1926232464} & \frac{1488078047}{4494542416} & \frac{1494625759}{13483627248} \end{bmatrix}, \begin{bmatrix} \frac{52104049}{120389529} & \frac{681707773}{481558116} & \frac{681707773}{481558116} \\ \frac{-71233997}{481558116} & \frac{-164964803}{1123635604} & \frac{-494924650}{842726703} \\ \frac{-71233997}{481558116} & \frac{-494924650}{842726703} & \frac{-164964803}{1123635604} \end{bmatrix},
$$

$$
\begin{bmatrix} \frac{1668011164}{842726703} & \frac{-40250807}{3370906812} & \frac{-40250807}{3370906812} \\ \frac{-40250807}{3370906812} & \frac{1668011164}{842726703} & \frac{-40250807}{3370906812} \\ \frac{-40250807}{3370906812} & \frac{-40250807}{3370906812} & \frac{1668011164}{842726703} \end{bmatrix},
$$

$$
\begin{bmatrix} \frac{-10815353}{9260733} & \frac{-20302895}{37042932} & \frac{-20302895}{37042932} \\ \frac{489004135}{481558116} & \frac{734318841}{1123635604} & \frac{179538083}{842726703} \\ \frac{489004135}{481558116} & \frac{179538083}{842726703} & \frac{734318841}{1123635604} \end{bmatrix}, \begin{bmatrix} \frac{20302895}{24695288} & 0 & 0 \\ \frac{-417301265}{642077488} & \frac{-37}{336} & \frac{37}{336} \\ \frac{-417301265}{642077488} & \frac{37}{336} & \frac{-37}{336} \end{bmatrix},
$$

$\widetilde{\mathbf{A}}_{(0,1)}$ and $\widetilde{\mathbf{A}}_{(1,1)}$ are given by

$$\begin{bmatrix} \frac{734318841}{1123635604} & \frac{489004135}{481558116} & \frac{179538083}{842726703} \\ \frac{-20302895}{37042932} & \frac{-10815353}{9260733} & \frac{-20302895}{37042932} \\ \frac{79538083}{842726703} & \frac{489004135}{481558116} & \frac{734318841}{1123635604} \end{bmatrix}, \begin{bmatrix} \frac{-164964803}{1123635604} & \frac{-494924650}{842726703} & \frac{-71233997}{481558116} \\ \frac{-494924650}{842726703} & \frac{-164964803}{1123635604} & \frac{-71233997}{481558116} \\ \frac{681707773}{481558116} & \frac{681707773}{481558116} & \frac{52104049}{120389529} \end{bmatrix},$$

and finally $\widetilde{\mathbf{A}}_{(0,2)}$ and $\widetilde{\mathbf{A}}_{(2,2)}$ are given by

$$\begin{bmatrix} \frac{-37}{336} & \frac{-417301265}{642077488} & \frac{37}{336} \\ 0 & \frac{20302895}{24695288} & 0 \\ \frac{37}{336} & \frac{-417301265}{642077488} & \frac{-37}{336} \end{bmatrix}, \begin{bmatrix} \frac{1494625759}{13483627248} & \frac{1488078047}{4494542416} & \frac{-212816425}{1926232464} \\ \frac{1488078047}{4494542416} & \frac{1494625759}{13483627248} & \frac{-212816425}{1926232464} \\ \frac{-366180055}{481558116} & \frac{-366180055}{481558116} & \frac{366180055}{963116232} \end{bmatrix}.$$

The dual symbol $\widetilde{P}(\omega)$ satisfies Condition E and we compute in MAPLE that $\widetilde{s} := -\frac{d}{2}\log_m \widetilde{\rho}$ equals $-0.431898...$, with $\widetilde{\rho} := \max\{|\nu| : \nu \in \mathrm{spec}(T_{\widetilde{P}}|_{\mathbb{H}})\}$. From Theorem 4.4 we find that the multilevel system $\mathbf{\Psi}$ is a Riesz basis for $H^s(\mathbb{R}^2)$ for all $s \in (0.431898..., \frac{5}{2})$. We do not have a Riesz basis for L_2.

5.4 Optimization on uniform grids

The previous lifting constructions are general in the sense that they apply to non-uniform meshes of arbitrary topological type. The lifting coefficients from local semiorthogonal lifting vary with the underlying non-uniform mesh. For many applications it is however sufficient to work on uniform grids. In such a case all lifting computations can be done in advance, and smarter ways exist to construct wavelets, see, e.g., [15, 16, 17]. The lifting scheme allows us to create wavelets with certain properties such as vanishing moments, symmetry, etc. The remaining degrees of freedom can be chosen in such a way that the range of stability is as large as possible by solving a minimization problem. Let us demonstrate this principle with an example. Consider the piecewise Hermite cubics from Section 5.2. The update stencil for the wavelets is as in Figure 9, so we get

$$\Psi(x) = \Phi(2x-1) - \begin{bmatrix} \alpha_1 & \alpha_2 \\ \beta_1 & \beta_2 \end{bmatrix} \Phi(x) - \begin{bmatrix} \alpha_3 & \alpha_4 \\ \beta_3 & \beta_4 \end{bmatrix} \Phi(x-1).$$

Suppose that we want two vanishing moments, ψ_1 has to be symmetric and ψ_2 has to be anti-symmetric. Then we need 6 degrees of freedom to satisfy these properties. Hence 2 degrees of freedom remain and the dual generator $\widetilde{\Phi}(x)$ satisfies the refinement equation

$$\begin{aligned} \widetilde{\Phi}(x) \;=\; & \begin{bmatrix} -\frac{9}{40} - \frac{\beta_2}{5} & -\frac{7}{60} - \frac{\beta_2}{15} \\ \alpha_2 + \frac{3\beta_2}{2} & \frac{\alpha_2+\beta_2}{2} \end{bmatrix} \widetilde{\Phi}(2x+2) + \begin{bmatrix} \frac{1}{2} & \frac{1}{30} - \frac{4\beta_2}{15} \\ -2\alpha_2 & 2\beta_2 \end{bmatrix} \widetilde{\Phi}(2x+1) \\ & + \begin{bmatrix} \frac{29}{20} + \frac{2\beta_2}{5} & 0 \\ 0 & 4 - \alpha_2 + \beta_2 \end{bmatrix} \widetilde{\Phi}(2x) \\ & + \begin{bmatrix} \frac{1}{2} & -\frac{1}{30} + \frac{4\beta_2}{15} \\ 2\alpha_2 & 2\beta_2 \end{bmatrix} \widetilde{\Phi}(2x-1) + \begin{bmatrix} -\frac{9}{40} - \frac{\beta_2}{5} & \frac{7}{60} + \frac{\beta_2}{15} \\ -\alpha_2 - \frac{3\beta_2}{2} & \frac{\alpha_2+\beta_2}{2} \end{bmatrix} \widetilde{\Phi}(2x-2) \end{aligned}$$

Theorems 4.3 and 4.4 characterize the range of stability, and Theorem 4.2 tells us how to compute the smoothness of $\widetilde{\Phi}(x)$. We use the minimization toolbox in MATLAB to compute the optimal values (i.e. those values that give the largest range of stability) for the two remaining degrees of freedom α_2 and β_2 . We find $\alpha_2 = \frac{11}{7}$ and $\beta_2 = -\frac{6}{11}$, or

$$\Psi(x) = \Phi(2x-1) - \begin{bmatrix} \frac{1}{4} & \frac{11}{7} \\ -\frac{59}{660} & -\frac{6}{11} \end{bmatrix} \Phi(x) - \begin{bmatrix} \frac{1}{4} & -\frac{11}{7} \\ \frac{59}{660} & -\frac{6}{11} \end{bmatrix} \Phi(x-1).$$

These wavelets are stable for $H^s(\mathbb{R})$ with $-0.828823 < s < 2.5$. Figure 14 visualizes the constructed functions. Note that these cubic Hermite spline wavelets are similar to the ones constructed in [8].

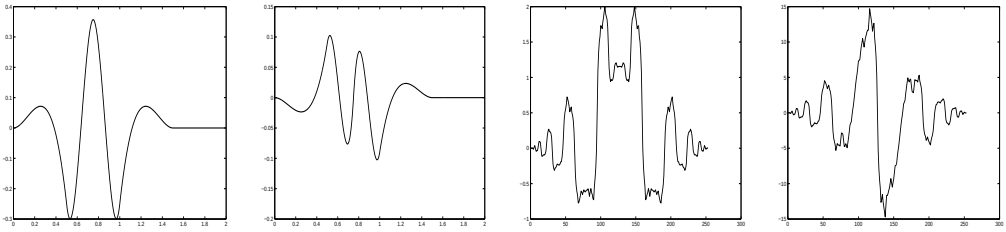

ψ_1 ψ_2 $\widetilde{\phi}_1$ $\widetilde{\phi}_2$

Figure 14: Cubic Hermite spline wavelet on $\mathbb{R}$

We conclude with a last example. Let us try to construct linear wavelets in $\mathbb{R}^2$ on the hexagonal lattice. We want them to have two vanishing moments, and we want hexagonal symmetry. If we use the same setting as in Section 5.1, then we initially have

$$\psi_{j,\lambda} = \phi_{j+1,\lambda} - \alpha_1 \phi_{j,\gamma_1} - \alpha_2 \phi_{j,\gamma_2} - \alpha_3 \phi_{j,\gamma_3} - \alpha_4 \phi_{j,\gamma_4}.$$

After some straightforward algebra we find that, in order to satisfy our wish list, we need three degrees of freedom out of four. Hence we keep one degree of freedom to stabilize our wavelet. The dual $\widetilde{\Phi}(x)$ satisfies

$$\begin{aligned} \widetilde{\Phi}(x) &= (4 - 12\alpha_1)\widetilde{\Phi}(Mx) + 4\alpha_1 \sum_{k \in K_1} \widetilde{\Phi}(Mx - k) + (2\alpha_1 - \frac{1}{2}) \sum_{k \in K_2} \widetilde{\Phi}(Mx - k) \\ &\quad + (\frac{1}{2} - 4\alpha_1) \sum_{k \in K_3} \widetilde{\Phi}(Mx - k), \ x \in \mathbb{R}^2. \end{aligned}$$

The optimal value for α_1 is computed with the optimization toolbox of MATLAB and we find $\alpha_1 = \frac{3}{16}$. The resulting wavelet

$$\psi_{j,\lambda} = \phi_{j+1,\lambda} - \frac{3}{16}(\phi_{j,\gamma_1} + \phi_{j,\gamma_2}) + \frac{1}{16}(\phi_{j,\gamma_3} + \phi_{j,\gamma_4})$$

is the same as the one constructed in [5] and the multilevel basis is a stable basis for $H^s(\mathbb{R}^2)$ with $-0.440765 < s < 1.5$.

Obviously in such situations one needs to be able to compute the spectral radius of the transition operator in an efficient way. One can for instance take into account the symmetry of the mask to optimize the computations. We refer to [13, 16] for more details.

Acknowledgements

This work is partially supported by the Flemish Fund for Scientific Research (FWO Vlaanderen) projects MISS (G.0211.02) and SMID (G.0431.05), and by the Belgian Programme on Interuniversity Attraction Poles, initiated by the Belgian Federal Science Policy Office. The scientific responsibility rests with the authors.

References

[1] R. A. Adams. *Sobolev spaces.* Academic Press, New York, 1975.

[2] J. H. Bramble, J. E. Pasciak, and J. Xu. Parallel multilevel preconditioners. *Math. Comp.*, 55:1–22, 1990.

[3] J. M. Carnicer, W. Dahmen, and J. M. Peña. Local decomposition of refinable spaces. *Appl. Comp. Harm. Anal.*, 3:127–153, 1996.

[4] A. Cohen and I. Daubechies. A new technique to estimate the regularity of refinable functions. *Rev. Mat. Iberoamericana*, 12(2):527–591, 1996.

[5] A. Cohen and J.-M. Schlenker. Compactly supported bidimensional wavelet bases with hexagonal symmetry. *Constr. Approx.*, 9:209–236, 1993.

[6] W. Dahmen. Some remarks on multiscale transformations, stability and biorthogonality. In P. J. Laurent, A. Le Méhauté, and L. L. Schumaker, editors, *Curves and surfaces*. Academic Press, 1994.

[7] W. Dahmen. Stability of multiscale transformations. *J. Fourier Anal. Appl.*, 4:341–362, 1996.

[8] W. Dahmen, B. Han, R.-Q. Jia, and A. Kunoth. Biorthogonal multiwavelets on the interval: Cubic Hermite splines. *Constr. Approx.*, 16:221–259, 2000.

[9] W. Dahmen and A. Kunoth. Multilevel preconditioning. *Numer. Math.*, 63:315–344, 1992.

[10] W. Dahmen, P. Oswald, and X.-Q. Shi. C^1-hierarchical bases. *J. Comput. Appl. Math.*, 51:37–56, 1994.

[11] I. Daubechies. *Ten Lectures on Wavelets*. SIAM, Philadelphia, 1992.

[12] O. Davydov and R. Stevenson. Hierarchical Riesz bases for $H^s(\Omega)$, $1 < s < 5/2$. *Constr. Approx.*, 22(3):365–394, 2005.

[13] B. Han. Computing the smoothness exponent of a symmetric multivariate refinable function. *SIAM J. Matrix Anal. Appl.*, 24:693–714, 2003.

[14] B. Han and R.-Q. Jia. Multivariate refinement equations and convergence of subdivision schemes. *SIAM J. Math. Anal.*, 29:1177–1199, 1998.

[15] B. Han, S. G. Kwon, and S. S. Park. Riesz multiwavelet bases. *Appl. Comput. Harmon. Anal.*, 20:161–183, 2006.

[16] B. Han, M. L. Overton, and T. Yu. Design of Hermite subdivision schemes aided by spectral radius optimization. *SIAM J. Sci. Comput.*, 25:643–656, 2003.

[17] Bin Han. Approximation properties and construction of Hermite interpolants and biorthogonal multiwavelets. *Journal of Approximation Theory*, 110(1):18–53, 2001.

[18] S. Jaffard. Wavelet methods for fast resolution of elliptic problems. *SIAM J. Numer. Anal.*, 29(4):965–986, 1992.

[19] R.-Q. Jia and Q. Jiang. Spectral analysis of the transition operator and its applications to smoothness analysis of wavelets. *SIAM J. Matrix Anal. Appl.*, 24:1071–1109, 2003.

[20] Q. Jiang. Multivariate matrix refinable functions with arbitrary matrix dilation. *Trans. Amer. Math. Soc.*, 351:2407–2438, 1999.

[21] Q. Jiang and P. Oswald. On the analysis of $\sqrt{3}$-subdivision schemes. Preprint, 2003.

[22] Q. Jiang and P. Oswald. Triangular $\sqrt{3}$-subdivision schemes: the regular case. *J. Comput. Appl. Math*, 156:47–75, 2003.

[23] W. Lawton, S. L. Lee, and Z. Shen. Convergence of multidimensional cascade algorithms. *Numer. Math.*, 78:427–438, 1998.

[24] R. Lorentz and P. Oswald. Criteria for hierarchical bases in Sobolev spaces. *Appl. Comput. Harm. Anal.*, 8:32–85, 2000.

[25] M. Lounsbery. *Multiresolution Analysis for Surfaces of Arbitrary Topological Type*. PhD thesis, University of Washington, Department of Computer Science and Engineering, 1994.

[26] M. Lounsbery, T. D. DeRose, and J. Warren. Multiresolution analysis for surfaces of arbitrary topological type. *ACM Trans. on Graphics*, 16(1):34–73, 1997.

[27] J. Maes and A. Bultheel. Stable multiresolution analysis on triangles for surface compression. *Electr. Trans. Numer. Anal.*, 25:224–258, 2006.

[28] P. Oswald. Hierarchical conforming finite element methods for the biharmonic equation. *SIAM J. Numer. Anal.*, 29:1610–1625, 1992.

[29] P. Oswald. Multilevel solvers for elliptic boundary value problems on domains. In W. Dahmen, A. J. Kurdila, and P. Oswald, editors, *Multiscale Wavelet Methods for Partial Differential Equations*, volume 6, pages 3–58. Academic Press, San Diego, 1997.

[30] G. Plonka and V. Strela. From wavelets to multiwavelets. In *Mathematical Methods for Curves and Surfaces II*. Vanderbilt University Press, Nashville, TN, 1998.

[31] M. J. D. Powell and M. A. Sabin. Piecewise quadratic approximations on triangles. *ACM Trans. on Math. Software*, 3:316–325, 1977.

[32] A. Ron and Z. Shen. The Sobolev regularity of refinable functions. *J. Approx. Theory*, 106:185–225, 2000.

[33] Z. Shen. Refinable function vectors. *SIAM J. Math. Anal.*, 29:235–250, 1998.

[34] J. Simoens and S. Vandewalle. A stabilized lifting construction of wavelets on irregular meshes on the interval. *SIAM J. Sci. Comput.*, 24(4):1356–1378, 2002.

[35] J. Stöckler. Multivariate wavelets. In C. K. Chui, editor, *Wavelets: A Tutorial in Theory and Applications*, pages 325–355. Academic Press, Boston, 1992.

[36] W. Sweldens. The lifting scheme: A custom-design construction of biorthogonal wavelets. *Appl. Comput. Harmon. Anal.*, 3(2):186–200, 1996.

[37] W. Sweldens. The lifting scheme: A construction of second generation wavelets. *SIAM J. Math. Anal.*, 29(2):511–546, 1997.

[38] E. Vanraes and A. Bultheel. Modeling sharp features with tangent subdivision. In M. Dæhlen, K. Marken, and L. Schumaker, editors, *Mathematical methods for curves and surfaces, Tromsø 2004*, pages 363–372. Nashboro Press, 2005.

[39] E. Vanraes and A. Bultheel. Tangent subdivision scheme. *ACM Trans. Graphics*, 25(2):340–355, 2006.

[40] P. S. Vassilevski and J. Wang. Stabilizing the hierarchical basis by approximate wavelets I: Theory. *Num. Lin. Alg. Appl.*, 4(2):103–126, 1997.

[41] P. S. Vassilevski and J. Wang. Stabilizing the hierarchical basis by approximate wavelets II: Implementation and numerical results. *SIAM J. Sci. Comput.*, 20:490–514, 1999.

[42] J. Windmolders and P. Dierckx. Subdivision of Uniform Powell–Sabin splines. *Comput. Aided Geom. Design*, 16:301–315, 1999.

[43] H. Yserentant. On the multi-level splitting of finite element spaces. *Numer. Math.*, 49:379–412, 1986.